Mon. Not. R. Astron. Soc. **297,** 579–616 (1998)

The stellar content of active galaxies

Roberto Cid Fernandes, Jr,[1⋆] Thaisa Storchi-Bergmann[2⋆†] and Henrique R. Schmitt[2⋆‡]

[1]*Departamento de Física, CFM - UFSC, Campus Universitário - Trindade, Caixa Postal 476, CEP: 88040-900 Florianópolis, SC, Brazil*
[2]*Instituto de Física - UFRGS, Caixa Postal 15051, CEP: 91501-970 Porto Alegre, RS, Brazil*

Accepted 1998 February 10. Received 1998 February 10; in original form 1997 February 11

ABSTRACT

We present the results of a long-slit spectroscopic study of 38 active and four normal galaxies. Stellar absorption features, continuum colours and their radial variations are analysed in an effort to characterize the stellar population in these galaxies and detect the presence of a featureless continuum underlying the starlight spectral component. Spatial variations of the equivalent widths of conspicuous absorption lines and continuum colours are detected in most galaxies. Star-forming rings, in particular, leave clear fingerprints in the equivalent widths and colour profiles. We find that the stellar populations in the inner regions of active galaxies present a variety of characteristics, and cannot be represented by a single starlight template. Dilution of the stellar lines by an underlying featureless continuum is detected in most broad-lined objects, but little or no dilution is found for most of the 20 type 2 Seyferts in the sample. Colour gradients are also ubiquitous. In particular, all but one of the observed Seyfert 2s are redder at the nucleus than in its immediate vicinity. Possible consequences of these findings are briefly outlined.

Key words: galaxies: active – galaxies: general – galaxies: nuclei – galaxies: Seyfert – galaxies: stellar content.

1 INTRODUCTION

Starlight constitutes a substantial fraction of the light gathered in optical spectra of active galactic nuclei (AGN), particularly in low-luminosity objects such as LINERs and Seyfert galaxies, where the stellar component is often dominant. To quantify and remove the contribution of the stellar population is one of the first and most critical steps in the analysis of AGN spectra, as the shape of the resulting continuum is strongly dependent on the adopted stellar population spectrum.

The most widely used technique for starlight subtraction consists of using an appropriately chosen spectrum of a normal galaxy as a template for the stellar component. The template spectrum is scaled to match as closely as possible the stellar absorption features in the observed spectrum, and the residual after its subtraction is taken as the stellar-free, pure AGN spectrum. This technique has been extensively applied since it was first introduced by Koski (1978), in his early study of Seyfert 2s (e.g. Stauffer 1982; Phillips, Charles & Baldwin 1983; Malkan & Filippenko 1983; Filippenko & Sargent 1988, 1985; Miller & Goodrich 1990; Ho, Filippenko & Sargent 1993; Kay 1994; Tran 1995a). Alternatively, the shape and strength of the starlight component can be estimated by means of stellar population synthesis techniques. This approach was followed by Keel (1983), who built synthetic templates using a library of stellar spectra plus assumptions about the mass function and star formation history. Synthetic templates can also be obtained by combining a spectral library of star clusters, a method first used by Bica (1988) in his analysis of the stellar populations of normal galaxies. Bonatto, Bica & Alloin (1989) and Storchi-Bergmann, Bica & Pastoriza (1990) used this technique to determine the integrated stellar content of the bulge of active galaxies.

The starlight evaluation procedure yields the stellar and AGN fluxes as a function of wavelength. The AGN spectrum, of course, is not known a priori, but the starlight subtraction is usually done in such a way as to produce a smooth residual continuum. This assumption is based on the fact that the continuum is essentially featureless in objects like bright Seyfert 1s and QSOs, where the AGN component dominates. It is customary to characterize the relative intensity of the starlight and featureless continuum (hereafter FC) components by their fractions ($f_\star$ and $f_{\rm FC}$) of the total flux at a given wavelength. These fractions depend on the chosen template, the aperture and the actual contrast between the AGN and stellar spectral components. The effect of the FC is to *dilute* the stellar absorption lines in the nuclear spectrum, and it is precisely the degree of dilution with respect to the starlight template that determines $f_\star$ and $f_{\rm FC}$.

In this paper we explore a different approach to estimate the dilution of absorption lines caused by the presence of an FC. Our

⋆E-mail: cid@fsc.ufsc.br (RCF); thaisa@if.ufrgs.br (TSB); schmitt@if.ufrgs.br (HRS)
†Visiting Astronomer, Cerro Tololo Interamerican Observatory.
‡CNPq fellow.

Table 1. Column (5) gives the activity class of the galaxy, where SB means starburst. Column (7) gives the radial velocity relative to the local group (in km s^{-1}), while column (8) lists the total blue magnitude of the galaxy and column (9) contains the foreground Galactic value of $E(B-V)$ (extracted from the Nasa Extragalactic Database).

SAMPLE PROPERTIES

NAME	ALT. NAME	α (1950)	δ (1950)	TYPE	MORPH.	v	B_{T_o}	$E(B-V)_G$
Mrk 348	NGC 262	00 46 05	31 41 04	2	SA(s)0/a	4669	13.94	0.060
3C 33	PKS 0106+13	01 06 12	13 02 33	NLRG	E	17230	19.50	0.025
NGC 526a	ESO 352-IG66	01 21 37	−35 19 32	1.9	S0 pec	5762	14.50	0.000
Mrk 573	UGC 1214	01 41 23	02 05 56	2	$SAB(rs)0^+$	5161	13.57	0.008
IC 1816	ESO 355-G25	02 29 48	−36 53 29	2	SA:(r:)a	5086	13.66	0.000
NGC 1097	ESO 416-G20	02 44 11	−30 29 01	Lin-1	SB(r l)b	1193	9.92	0.020
ESO 417-G6	MCG-05-08-006	02 54 18	−32 23 00	2	(R)SA0/a	4792	14.15	0.000
NGC 1326	ESO 357-G026	03 22 01	−36 38 24	Lin	SB(rl)0/a	1244	11.25	0.000
Mrk 607	NGC 1320	03 22 18	−03 13 03	2	Sa:sp	2716	13.31	0.018
NGC 1358	MCG-1-10-003	03 31 11	−05 15 24	2	SAB(r)0/a	3980	12.70	0.025
NGC 1386	ESO 358-G35	03 34 51	−36 09 47	2	$SB(s)0^+$	741	12.12	0.000
NGC 1433	ESO 249-G014	03 40 27	−47 22 48	Lin	SB(rs)ab	920	11.37	0.000
PKS 0349−27	GSP 022	03 49 32	−27 53 29	NLRG	E	19190	16.80	0.000
NGC 1598	ESO 202-G26	04 27 08	−47 53 29	Lin	SAB(s)c	4939	13.44	0.000
NGC 1672	ESO 118-G043	04 44 55	−59 20 18	Lin	SB(r)bc	1155	10.25	0.000
CGCG 420-015		04 50 47	03 58 47	2	E/S0	8811	15.00	0.070
ESO 362-G8	MCG-06-12-009	05 09 20	−34 27 12	2	S0?	4616	13.51	0.005
ESO 362-G18	MCG-05-13-017	05 17 44	−32 42 30	1	S0/a	3603	13.58	0.000
Pictor A	ESO 252-GA018	05 18 24	−45 49 43	BLRG	$SA0^0$:pec	10308	15.94	0.225
PKS 0634−20	IRAS 06343−2032	06 34 24	−20 32 19	NLRG	E	16320	17.58	0.405
PKS 0745−19		07 45 17	−19 10 15	NLRG	E	35940	18.00	—
Mrk 1210	UGC 4203	08 01 27	05 15 22	2	S?	3910	14.21	0.018
NGC 2935	ESO 565-G23	09 34 26	−20 54 12	Normal	SAB(s)b	2072	11.81	0.028
NGC 3081	ESO 499-IG31	09 57 10	−22 35 06	2	SAB(r)0/a	2164	12.59	0.033
Mrk 732	IC 2637	11 11 14	09 51 33	1.5	E pec	8670	13.89	0.005
IRAS 11215−2806		11 21 35	−28 96 46	2		4047	13.00	0.088
MCG-05-27-013		11 24 55	−28 59 00	2	SB(r)a?	7263	13.71	0.063
NGC 4303	UGC 7420	12 19 22	04 45 03	Lin	SAB(rs)bc	1486	13.68	0.000
MCG-02-33-034		12 49 35	−13 08 36	1		4386	15.00	0.015
Fairall 316	ESO 269-G12	12 53 50	−46 39 18	2	S0?	4772	13.81	0.185
NGC 5135	ESO 444-G32	13 22 57	−29 34 26	2-SB	SB(l)ab	3959	12.37	0.058
NGC 5248	UGC 8616	13 35 02	09 08 23	Normal	SAB(rs)bc	1128	10.63	0.000
NGC 5643	ESO 272-G16	14 29 28	−43 57 12	2	SAB(rs)c	1066	10.23	0.125
NGC 6221	ESO 138-G03	16 48 26	−59 08 00	SB	SB(s)bc pec	1368	9.77	0.220
NGC 6300	ESO 101-G25	17 12 18	−62 45 54	2	SB(rs)b	997	10.20	0.120
NGC 6814	MCG-02-50-001	19 39 56	−10 26 33	1	SAB(rs)bc	1676	10.96	0.150
IC 4889	ESO 185-G14	19 41 18	−54 27 54	Normal	E	2473	12.06	0.045
NGC 6860	ESO 143-G09	20 04 29	−61 14 42	1	SB(r)ab	4385	13.68	0.020
NGC 6890	MCG-07-41-023	20 14 49	−44 57 48	2	SB(r)ab	2459	12.82	0.008
NGC 7130	IC 5135	21 45 20	−35 11 07	2-SB	Sa pec	4850	12.88	0.000
NGC 7213	ESO 288-G43	22 06 08	−47 24 45	Lin-1	$SA(s)0^0$	1767	11.13	0.000
NGC 7582	ESO 291-G16	23 15 38	−42 38 36	2-SB	SB(s)ab	1551	10.83	0.000

method makes use of the radial information available through high signal-to-noise-ratio (S/N) long-slit spectroscopy of a large sample of objects. By studying the variation of the equivalent width (W) of conspicuous absorption lines as a function of distance to the nucleus, we are able to determine how much dilution (if any) occurs in the nucleus with respect to extra-nuclear regions, presumably not affected by the FC. In a way, this method amounts to using the off-nucleus spectrum of a galaxy as its own starlight template, a starlight evaluation technique which has been a successfully applied in some previous works (Fosbury et al. 1978; Schmitt, Storchi-Bergmann & Baldwin 1994; Winge et al. 1995; Storchi-Bergmann et al. 1997). Continuum colour gradients are also examined, complementing the study of absorption-line gradients and bringing in information about the reddening of the nuclear regions.

A second goal of this paper is to provide a homogeneous data base for the study of the stellar populations in active galaxies. As discussed above, in previous works the interest in the stellar population has focused on removing its contribution from the nuclear spectrum. The Ws and continuum colours measured in this work allow a characterization of the global properties of the stellar populations as close as a few hundred parsecs from the nucleus, offering the prospect of a comparative study between the stellar content of normal and active galaxies and between different types of AGN.

This investigation touches upon a number of key issues in current AGN research, such as: (1) the question of starlight evaluation and subtraction techniques; (2) the characterization of the stellar population in active galaxies; and (3) the nature of the FC in Seyfert 2 galaxies and its implications for unified models. In the current paper

Table 2. Details of the observations. Column (4) lists the slit position angle (PA). The parallactic angle (ϕ) is listed in column (6). Column (7) lists the pixel size in arcsec, while column (8) lists the spatial scale in pc arcsec^{-1}.

LOG OF OBSERVATIONS

NAME	DATE	EXP. TIME (sec)	PA [°]	AIR MASS	ϕ [°]	PIXEL	SCALE pc/arcsec	COMMENTS
Mrk 348	6/7 Dec. 94	1800	170	2.20	170	0.9	302	
3C 33	6/7 Dec. 94	1800	65	1.43	167	0.9	1114	
NGC 526a	5/6 Dec. 94	3600	124	1.02	69	0.9	372	
Mrk 573	6/7 Dec. 94	1800	125	1.64	131	0.9	334	
IC 1816	6/7 Jan. 94	1800	90	1.07	82	1	328	
NGC 1097	6/7 Jan. 94	1800	139	1.01	88	1	77	
ESO 417-G6	6/7 Dec. 94	3600	155	1.01	69	0.9	310	
NGC 1326	5/6 Jan. 94	1800	77	1.15	88	1	80	
Mrk 607	6/7 Jan. 94	900	135	1.22	140	1	176	
NGC 1358	6/7 Jan. 94	900	145	1.23	136	1	257	
NGC 1386	6/7 Jan. 94	1800	169	1.12	89	1	48	
NGC 1433	6/7 Dec. 94	1200	19	1.05	19	0.9	59	
PKS 0349−27	5/6 Dec. 94	3600	82	1.04	103	0.9	1240	
NGC 1598	6/7 Jan 94	1800	123	1.13	65	1	319	
NGC 1672	5/6 Jan 94	1800	94	1.32	63	1	75	
CGCG 420-015	6/7 Jan 94	900	40	1.46	140	1	570	
ESO 362-G8	6/7 Jan. 94	1800	165	1.17	88	1	298	
ESO 362-G18	6/7 Jan. 94	1800	55	1.19	82	1	233	
Pictor A	6/7 Dec. 94	1800	71	1.15	71	0.9	666	
PKS 0634−20	5/6 Dec. 94	3600	139	1.07	129	0.9	1055	
PKS 0745−19	6/7 Dec. 94	1800	150	1.03	149	0.9	2323	
Mrk 1210	5/6 Jan. 94	1800	163	1.25	163	1	253	
NGC 2935	5/6 Jan. 94	1800	0	1.02	182	1	134	
NGC 3081	28/29 May 92	1200	73	1.25	70	0.9	140	seeing 3 arcsec
Mrk 732	6/7 Jan. 94	1800	55	1.50	31	1	560	
IRAS 11215−2806	5/6 Jan. 94	900	145	1.02	76	1	262	
MCG-05-27-013	6/7 Jan. 94	1800	0	1.20	78	1	470	
NGC 4303	28/29 May 92	1800	112	1.69	50	0.9	96	
MCG-02-33-034	6/7 Jan. 94	1800	25	1.24	55	1	284	
Fairall 316	6/7 Jan. 94	1800	100	1.29	102	1	308	
NGC 5135	29/30 May 92	1800	30	1.25	100	0.9	256	
NGC 5248	28/29 May 92	1800	146	1.58	144	0.9	73	
NGC 5643	28/29 May 92	1800	90	1.19	75	0.9	69	
NGC 6221	28/29 May 92	1800	5	1.24	56	0.9	88	clouds
NGC 6300	28/29 May 92	1800	124	1.19	18	0.9	63	clouds
NGC 6814	29/30 May 92	1800	161	1.06	170	0.9	108	clouds
IC 4889	28/29 May 92	1800	0	1.12	29	0.9	160	clouds
NGC 6860	28/29 May 92	1800	70	1.21	36	0.9	283	clouds
NGC 6890	29/30 May 92	1800	153	1.03	12	0.9	159	clouds
NGC 7130	29/30 May 92	900	143	1.01	50	0.9	314	
NGC 7213	29/30 May 92	1200	50	1.04	0	0.9	114	
NGC 7582	6/7 Jan. 94	300	67	1.53	83	1	100	

we focus on the presentation of the data, the analysis of the stellar population features and their radial variations. Future communications will explore the consequences and interpretation of our results in full detail.

This paper is organized as follows. In Section 2 we present the sample galaxies and describe the observations. The method of analysis (continuum determination and W measurement) is discussed in Section 3. The results are presented in Section 4 and discussed in Section 5. Finally, Section 6 summarizes our main results.

2 OBSERVATIONS

The sample comprises 20 Seyfert 2s, six Seyfert 1s, seven LINERs and five radio galaxies, as well as four 'normal' nuclei. With the exception of the radio galaxies, all of them are bright nearby objects. Table 1 describes the sample properties. Long-slit spectra of these galaxies have been collected in three epochs, using the same technique and instrumentation, such that we have formed a homogeneous data base, which can be used for a comparative study of the different kinds of galaxies.

The observations were carried out using the Cassegrain spectrograph with the 4-m telescope of the Cerro Tololo Interamerican Observatory. The spectral range covered is ~3500–7000 Å, at a resolution of 5–8 Å. A slit width corresponding to 2 arcsec in the sky was oriented along the position angle (hereafter PA) that allowed the best coverage of the extended emission (although in this work we concentrate on the properties of the continua and stellar absorption features). A log of the observations is presented in Table 2, where we also list the parallactic angle, airmass during the

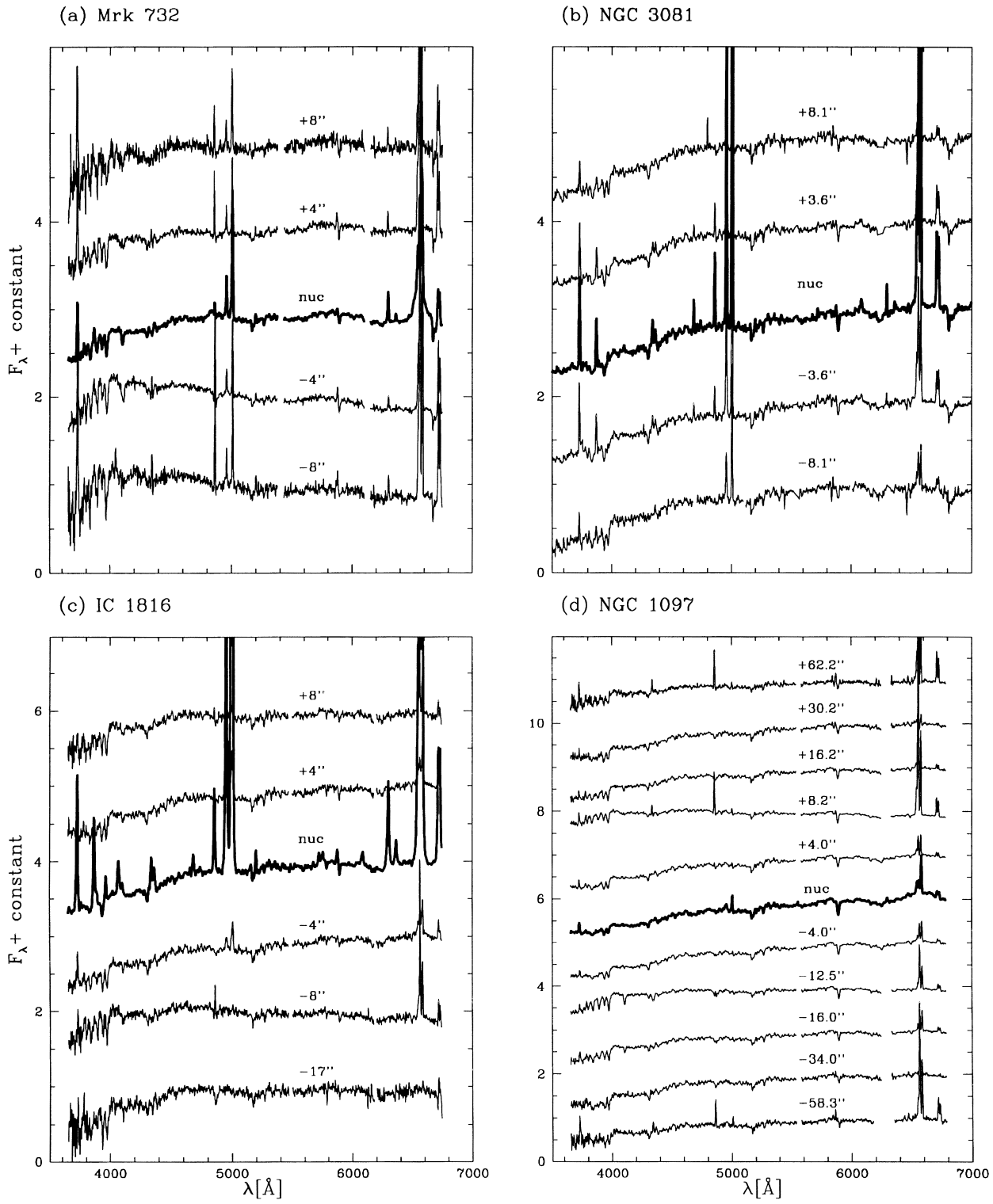

Figure 1. Selected examples of the spatially resolved spectra of four of the sample galaxies. The nuclear spectra are indicated by thick lines. The angular distances from the nuclei are indicated, positive values corresponding to a westerly (W, NW or SW) or southerly direction (in the case when the observed PA is 0°). The spectra are normalized at 5870 Å and shifted vertically by one unit to facilitate comparison. Residual sky emission lines have been removed.

observations, pixel size and spatial scale (evaluated with $H_0 = 75$ km s^{-1} Mpc^{-1}). It can be seen that only for a few galaxies, namely 3C 33, CGCG 420-015 and NGC 4303, is the effect of differential refraction important, displacing the light at 3700 Å by ~1 arcsec relative to the light at 5000 Å, so that some distortion of the continuum slope can be expected in the individual extractions for these objects, if the continuum presents significant variations along the slit. The reduction of the spectra was performed using standard techniques in IRAF. After flux and wavelength calibration, the redshifts were determined from the

narrow emission lines present and the spectra were converted to rest-frame units.

The long slit used corresponded to 5 arcmin in the sky, and sky subtraction was performed by fitting a polynomial to the outer regions of the frame and then subtracting its contribution to the whole frame using the task BACKGROUND in IRAF. The most extended galaxies, presenting enough S/N ratio to allow measure the spectral features up to approximately 100 arcsec, were NGC 1097, the most extended, followed by NGC 1672. For these galaxies the sky level adopted may have been overestimated. In order to evaluate an upper limit to the effect, we have compared the flux level of the adopted sky with the flux of the inner regions. We have concluded that its value amounts to less than 1 per cent when compared with the flux of the nucleus, but rises with distance from the nucleus. At approximately 25 arcsec, its contribution is about 10 per cent. Assuming that the 'sky' flux is actually galaxy flux, the flux level of the sky-subtracted spectrum will be underestimated by at most 10 per cent at 25 arcsec and more farther out. Thus the measurements of these two galaxies are subject to this uncertainty farther than 25 arcsec from the nucleus. The effect should be negligible for the other less extended galaxies.

One-dimensional spectra were extracted from the two-dimensional frames. The number of extractions varied from four for PKS 0745−19 to as many as 26 for NGC 1097, totalling 491 spectra for the whole sample. The spatial coverage ranged between ±3 and ±80 arcsec from the nucleus, while the width of the extractions was typically 2 arcsec in the brighter nuclear regions, gradually increasing towards the fainter outer regions to guarantee enough signal. Given that the seeing during the observations was typically 1.5 arcsec, some of the narrow extractions are slightly oversampled, resulting in a smoothing of the sharpest spectral variations.

The S/N ratio at 5650 Å ranges from ∼ 5 to 100, with an average of 40 for all extractions. Even in the blue region, where the noise is usually higher, the spectra are of excellent quality, with a mean S/N ratio of 25 at 4200 Å. The high quality of our data has allowed the measurement of stellar population features in spectra extracted up to several kiloparsecs from the nuclei. There is no similar data base with this quality for so many galaxies in the literature.

Fig. 1 shows representative spectra of four of the sample galaxies for several positions along the slit. Note that absorption features are well detected in all spectra, as well as variations of spectral characteristics with distance from the nuclei. Signatures of young stellar populations, in particular, are clearly present in several of the spectra shown: over the whole inner 8 arcsec of Mrk 732, more conspicuously at 4 arcsec north-east ($r = -4$ arcsec in Fig. 1); at ∼8 arcsec from the nucleus in IC 1816, and at ∼8–12 arcsec in NGC 1097 (corresponding to the locus of the nuclear ring: Storchi-Bergmann, Wilson & Baldwin 1996a). Further examples of the spatially resolved spectra are shown in Fig. 45 (see later).

3 METHOD OF ANALYSIS

Our main goal is to study the run of the stellar absorption features with distance from the nucleus. To this end, the analysis of each of the sample spectra consisted of (1) determining the 'pseudo'-continuum at selected pivot-points (3780, 4020, 4510, 4630, 5313, 5870 and 6080 Å) and (2) measuring the equivalent widths of the Ca II K and H, CN, G-band, Mg I+Mg H and Na I absorption lines, integrating the flux with respect to the pseudo-continuum.

The continuum and W measurements followed the method outlined by Bica & Alloin (1986), Bica (1988) and Bica, Alloin & Schmitt (1994), and subsequently used in several studies of both normal and emission-line galaxies (e.g. Bonatto et al. 1989; Storchi-Bergmann et al. 1990; Jablonka, Alloin & Bica 1990; Storchi-Bergmann, Kinney & Challis 1995b; McQuade, Calzetti & Kinney 1995). This method consists of determining a pseudo-continuum at a few pivot-wavelengths and integrating the flux difference with respect to this continuum in pre-defined wavelength windows (Table 3) to determine the Ws. The pivot-wavelengths used in this work are based on those used by the above authors and were chosen to avoid, as much as possible, regions of strong emission or absorption features. The use of a compatible set of pivot-points and wavelength windows is important because it will allow a detailed quantitative analysis of the stellar population – via synthesis techniques using Bica's (1988) spectral library of star clusters – to be presented in a forthcoming paper. Here we will use our measurements only to look for broad trends in the properties of the stellar populations, and to identify signs of a nuclear FC (see below).

Table 3. Wavelength windows used to measure the equivalent widths of the absorption lines.

LINE	WINDOWS
Ca II K	3908–3952
Ca II H+Hϵ	3952–3988
CN	4150–4214
G band	4284–4318
Mg I+Mg H	5156–5196
Na I	5880–5914

The determination of the continuum has to be done interactively, taking into account the flux level, the noise and minor wavelength calibration uncertainties as well as anomalies due to the presence of emission lines. The 5870- and 6080-Å points, in particular, are sometimes buried underneath He I 5876- and [Fe VII]6087-Å emission lines (for instance, in the nuclear regions of IC 1816, Mrk 348 and NGC 3081). In such cases the placement of the continuum was guided by adjacent wavelength regions. In a few cases, it was also necessary to make 'cosmetic' corrections when a noise spike was present in the wavelength window used to compute the W. We emphasize, however, that such anomalies were very rare. In the majority (> 90 per cent) of cases the excellent quality of the spectra allowed a precise determination of the continua and Ws.

Fig. 2 illustrates the application of the method to four of the sample spectra. The spectrum in Fig. 2(a) corresponds to the nucleus of the LINER NGC 1598. The spectrum is almost purely stellar, posing no difficulties to the determination of the pseudo-continuum. Note that the continuum runs well above the actual spectrum except at the pivot-points. Fig. 2(b) shows the nuclear spectrum of Mrk 348, a type 2 Seyfert. Here, as for all Seyfert 2s in the sample, the continuum can still be placed with little ambiguity, despite the presence of many emission lines. As in many other cases, the Ca H line is filled with [Ne III] and Hϵ emission in the central regions, but not at the outer positions, an effect which must be taken into account when interpreting W(Ca H) spatial gradients. Note also that, as in Fig. 2(d), the 5870- and 6080-Å points are underneath He I and [Fe VII] emission, respectively. This is not a problem, as the continuum can still be determined from the adjacent regions.

Whilst for most LINERs, Seyfert 2s and normal galaxies the placement of the continuum is straightforward, this is not the case in

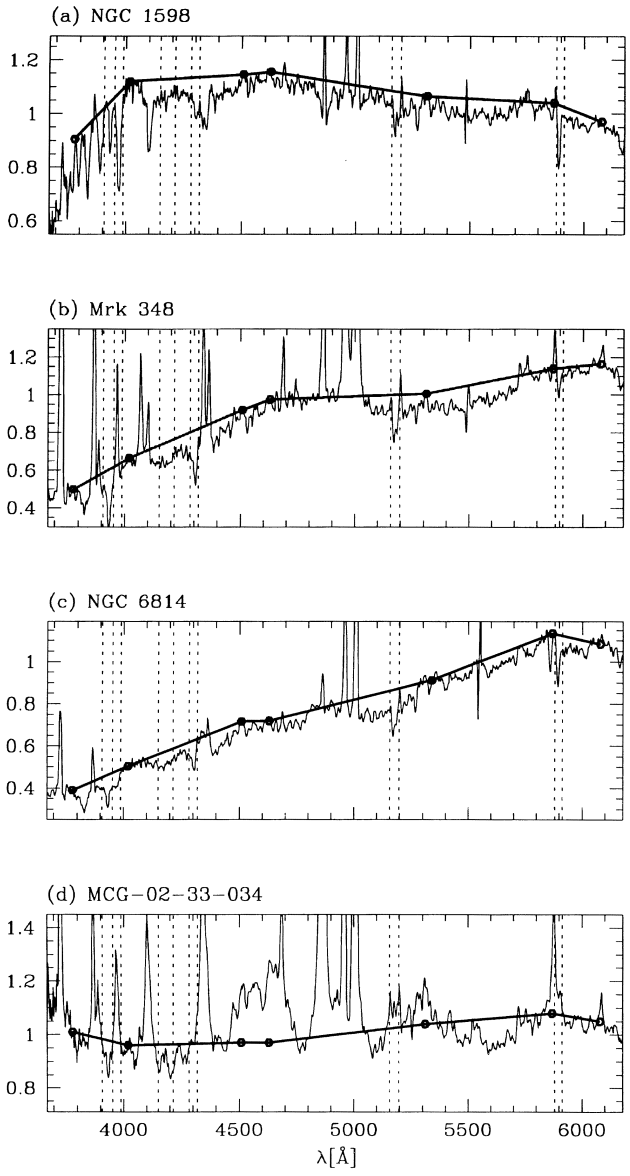

Figure 2. Illustration of the continuum determination procedure for the nuclear spectra of the LINER NGC 1598 (a), the Seyfert 2 Mrk 348 (b), and the Seyfert 1 galaxies NGC 6814 (c) and MCG-02-33-034 (d). The continuum pivot-points are marked by the filled circles. Dashed vertical lines indicate the wavelength windows used to measure the equivalent widths of Ca K and H, CN, G-band, Mg and Na lines.

the nuclear regions of strong Seyfert 1s, where the numerous broad lines and intense non-stellar continuum complicate the analysis. This is illustrated in Fig. 2(d), where we plot the nuclear spectrum of MCG-02-33-034. The 4510-, 4630- and 5313-Å points, in particular, are all underneath Fe II blends, making it impossible to determine them accurately. None of the absorption lines in Fig. 2(d), with the possible exception of Ca K, is free of contamination. The Mg line, for instance, is filled up by Fe II and [N I]5200-Å emission, while the Na window is contamined by broad He I 5876 Å. It is clear that in extreme cases like this no reliable values for the Ws of the absorption lines can be derived with our or any other method. The presence of such a strong nuclear FC should appear as a dip at $r = 0$ in the radial profiles of the Ws, and this is indeed seen in Fig. 7 (later). However, given the difficulties in defining a continuum, the depth of this dip is unreliable. At any rate, the only other galaxy in the present sample with a spectrum as complex as MCG-02-33-034 is the broad-line radio galaxy Pictor A (Fig. 32, later). For less extreme Seyfert 1s like NGC 6814 (Fig. 2c), the continuum can be defined with little ambiguity.

The four examples in Fig. 2 span essentially all types of spectra found in the sample. Overall, we found that the method works well for most spectra, with the exception of the nuclear regions of strong Seyfert 1s. The comparison of the Ws and continuum colours in the nuclear and outer regions is a useful tool with which to detect the presence of an FC, particularly in Seyfert 2s and LINERs, where the FC, if present, is not as conspicuous as in type 1 objects. Indeed, one of our major goals is to verify whether Seyfert 2s and LINERs exhibit signs of such a nuclear FC, which should cause a dilution of the absorption lines with respect to those measured outside the nucleus.

3.1 Consistency and error analysis

The positioning of the continuum can be somewhat subjective, particularly in the noisier spectra, given that it has to be carried out interactively. In order to verify whether our measurements are consistent with those of Bica (1988) we have measured the continuum fluxes and Ws of the 15 templates corresponding to his spectral groups E1–E8 and S1–S7. The difference between his and our continuum measurements is of the order of 1 per cent. For the Ws the difference is typically ≈0.5 Å and always smaller than 1 Å, corresponding to an agreement at the 5–10 per cent level. This compatibility is important, since it ensures that we can apply stellar population characterization techniques similar to those employed by Bica.

In the discussion of our results (Section 4) we will compare the Ws and continua of the galaxies in the present sample with templates S1 to S7 and E1 to E8 of Bica (1988) as a guide to obtaining a broad characterization of the stellar populations. (As pointed out in the previous section, a full quantitative analysis of the stellar populations will be presented in a forthcoming paper.) These templates correspond to increasing contributions of young components, from S1 and E1 to S7 and E8. Templates S1 to S3 and E1 to E6 are composed of old ($> 5 \times 10^9$ yr) and intermediate-age stars (5×10^8–10^9 yr), differing mostly in the contribution from stars of different metallicities. From S4 to S7 and E7 to E8 we have an increasing contribution from young stars ($< 10^8$ yr), which can reach as much as 65 per cent (for S7) and 20 per cent (for E8) of the flux at 5870 Å.

The Ws measured in this work are subject to two different sources of error: (1) the noise present in the spectra, and (2) the uncertainty in the placement of the continuum.

The error in the Ws due to noise was evaluated using standard propagation of errors. The noise level was computed from the rms dispersion in a 60–100 Å region free of strong emission or absorption lines. Two windows, one in the 4200-Å region and the other around 5650 Å, were used for this purpose. The noise in the first window was used to compute the errors in the Ws of Ca K and H, CN and the G band, whereas the latter window was used for the Mg and Na lines. The resulting errors are typically 0.5 Å for the 'blue' lines (Ca K to the G band), and 0.3 Å for Mg and Na. The errors in the central regions are usually smaller than these average values, since the noise is lower there. The Ca K line in NGC 7213, for instance, has an error of ∼0.3 Å in the central 5 arcsec, gradually increasing to ∼0.7 Å for $r > 22$ arcsec.

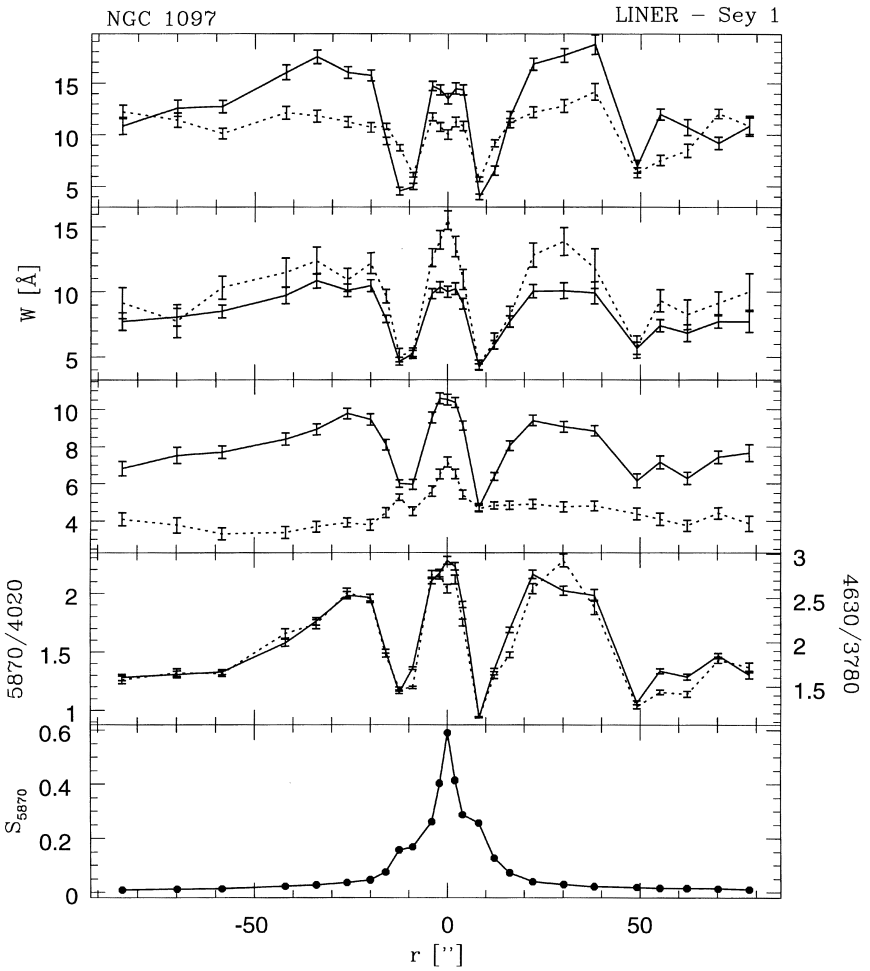

Figure 3. Radial variations of the equivalent widths (W), colours and surface brightnesses for NGC 1097. The upper panel plots the Ws of Ca II K (solid line) and Ca II H (dotted), while the second panel shows the G band (solid) and CN (dotted), and the third panel shows Mg I+Mg H (solid) and Na I (dotted). The fourth panel shows the radial variations of the continuum colours, mapped with the F_{5870}/F_{4020} (solid line, left-hand scale) and F_{4630}/F_{3780} (dotted line, right-hand scale) flux ratios. Red is up and blue is down in this plot. The bottom panel shows the run of the surface brightness at 5870 Å (in units of erg cm^{-2} s^{-1} Å^{-1} arcsec^{-2}) along the slit.

The uncertainties in the placement of the continuum are less straightforward to evaluate, since, as explained above, the continuum is not automatically defined, but determined interactively. To compute the error in the Ws associated with this source of uncertainty we re-analysed the spectra of four galaxies (42 extractions in total), defining upper and lower values of the continuum at the pivot-points. The mean difference between these values and the adopted one (all evaluated in the middle of the line window) was taken as a measure of the error in the continuum flux, which was then propagated to the Ws. We found that the resulting errors are typically 30–50 per cent larger than the errors due to noise alone. As expected, the uncertainty in the positioning of the continuum increases with decreasing S/N ratio. Since it is not practical to measure lower and upper continua for all 491 spectra, we have used this scaling between the S/N ratio and the continuum errors measured above to estimate the errors due to the positioning of the continuum for the remaining objects.

The combined error in the Ws due to noise and continuum positioning, added in quadrature, are typically 0.5 Å for Ca K, Ca H and the G band, 0.4 Å in Mg and Na, and 1.0 Å for the CN line. The larger error in the CN reflects the fact that this feature is very shallow, being essentially a measure of the local height of the pseudo-continuum above the actual spectrum. In fact, it is often difficult to identify the CN feature in the spectra (e.g. Fig. 2). Indeed, the CN band is pronounced only in very metal-rich populations, such as templates S1 and E1 of Bica (1988). We nevertheless keep this line in our analysis, since our measured Ws are consistent with those found by Bica and in most cases its radial variations follow those of the other absorption lines.

In the discussion of our results, we shall put more emphasis on the Ca K, G-band and Mg features, since the Ca H line is often contaminated by emission and the CN line is subject to larger errors. The Na line is not a good diagnostic of stellar population, since it is partially produced in the interstellar medium of the host galaxy. This line can, however, be used as an indication of the presence of dust (Bica & Alloin 1986; Bica et al. 1991). In the attribution of template types to the different spectra a larger weight is given to Ca K, since this is often the strongest line, less affected by errors. As discussed in Section 4.1, sometimes different lines indicate different template types, which simply indicates a different mixture of stellar populations than found in Bica's (1988) grid of spectral templates.

The uncertainty in the determination of the Ws limits the degree of dilution measurable from our data. The effect of an FC contributing a fraction f_{FC} of the total flux in a given wavelength is to decrease the W of an absorption line in this wavelength by this same factor: $\Delta W = f_{FC} W$. Therefore the minimum amount of dilution that can be safely measured from the radial variations of a line with a W of, say, 10 Å and an error of 0.5 Å is ~5 per cent. From the results presented in the next section we estimate that this method of evaluating the contribution of an FC works well for $f_{FC} \gtrsim 10$ per cent for the present data set as a whole, although smaller lower limits are reached in the best spectra.

4 RESULTS

The main results of the data analysis are presented in Figs 3–44, where we plot the radial variations of the Ws, colours and surface brightnesses for all the galaxies in the sample. In each figure, the top panel shows the Ws of Ca K (solid line) and Ca H (dotted) against the distance from the nucleus (r). Similarly, the second panel shows the Ws of the G band (solid) and CN (dotted), while the third panel shows Mg (solid) and Na (dotted). Negative values of the W indicate emission, as often found in the Ca H plots due to contamination by [Ne III] and Hϵ. The Mg and Na lines are also contaminated by emission in some cases. Apart from such cases (discussed in detail in Section 4.1), a dip in the W plots indicates dilution of the absorption lines by an FC or the presence of a young stellar population. The fourth panel shows the colour profiles, mapped by the ratios of the 5870- to 4020-Å (solid line) and 4630- to 3780-Å (dotted line) pseudo-continuum fluxes. (Note that the left-hand scale in this plot corresponds to F_{5870}/F_{4020}, whereas the values on the right correspond to F_{4630}/F_{3780}.) Dips in the colour plots indicate a blue continuum, whereas peaks indicate a red continuum, due to an old stellar population and/or reddening. The colours have been corrected by foreground galactic reddening using the values of $E(B-V)$ in Table 1. This correction, besides being small, does not affect the shape of the curves. Finally, to give a measure of the flux level in each position, the bottom panel shows the run of the surface brightness in the 5870-Å pseudo-continuum with distance from the nucleus.

In order to illustrate better the results presented in Figs 3–44, Fig. 45 shows the spatially resolved spectra of five galaxies, representing the five classes of objects studied, zoomed into the wavelength regions of the absorption lines analysed in this work. This figure also serves as a further illustration of the determination of the pseudo-continuum and of the quality of the current data base.

We start our discussion of the results with the cases of NGC 1097, 1433 and 1672. The presence of star-forming rings in these galaxies serves as a good illustration of the consistency of our measurements and as a guide to the interpretation of the W and colour gradients in other objects. NGC 1326, 2935, 4303 and 5248 also present star-forming rings, and much of the the discussion below also applies to these objects.

NGC 1097, a nearby spiral galaxy, has a low-luminosity nucleus, characterized by a LINER-like emission-line spectrum, surrounded by a ring of H II regions (Sérsic & Pastoriza 1965, 1967; Phillips et al. 1984). In addition to its LINER spectrum, the broad, double-peaked, variable Balmer lines in the nucleus of NGC 1097 are a clear signature of the presence of an active nucleus in this galaxy (Storchi-Bergmann, Baldwin & Wilson 1993; see Fig. 1). The low Ws and blue colours typical of the young stellar populations of the ring are remarkably well depicted in Fig. 3 by the dips at $|r| \sim 10$ arcsec in the radial profiles of the Ws and colours. Despite its active nucleus, the optical continuum shows little evidence of a blue FC of the kind found in type 1 Seyferts and QSOs. This is seen in Fig. 3, which shows that the Ws in the nucleus of NGC 1097 are not significantly diluted with respect to their values inside or outside the ring. On the contrary, the CN and Mg lines seem to be stronger in the nucleus than outside it, while the Na line clearly peaks at $r = 0$. The Ca K and H lines, however, do present a central dip, albeit of a low amplitude. Comparing the nuclear spectrum with the $r = -4$ and $+4$ arcsec extractions, we find variations of 7 and 11 per cent in the Ws of Ca K and H respectively (Section 5.2), which indicates that an AGN continuum, if present, contributes less than ~10 per cent of the light in this wavelength region. Considering that the error in these Ws is ~5 per cent, the evidence for a diluting FC in NGC 1097 is marginal.

The Ws in NGC 1097 can be represented by an S2–S3 template at the nucleus, S6–S7 at the ring and S3 farther out. The continuum ratios are consistent with the spectral templates inferred from the Ws, with the exception of the nuclear region, where the continuum is redder, more typical of an S1 template. This could be interpreted as evidence of reddening of the nuclear regions, as is also indicated by the increase of the W(Na) towards the nucleus (Storchi-Bergmann et al. 1995a). This difference in template types can be accounted for with $E(B-V) \approx 0.15$. Storchi-Bergmann et al. (1995b) obtained a large-aperture spectrum of this object (10×20 arcsec^2), including the nucleus and part of the star-forming ring. Their measured Ws can be represented by an S5 template, which is comparable to our results in the inner 10 arcsec. The *IUE* spectrum of NGC 1097 is dominated by the ring, showing several absorption lines typical of young stars (Kinney et al. 1993).

NGC 1433 has been classified as a Seyfert 2 by Véron-Cetty & Véron (1986), although our spectrum presents emission-line ratios more typical of LINERs. It also contains a star-forming ring ~8 arcsec from its nucleus (Buta 1986). As in the case of NGC 1097, the ring leaves a clear fingerprint in the W and colour profiles (Fig. 36). No dilution of the absorption lines or blueing of the continuum is seen in the nuclear spectrum. Both the Ws and continuum ratios indicate similar spectral templates: S3 at the nucleus, S5 at the ring and S3 farther out. As in NGC 1097, the general decrease of the Ws and bluer colours towards large distances seen in Fig. 36 correspond to the stellar population of the disc of the galaxy.

NGC 1672 is a Sersic–Pastoriza galaxy, the nucleus of which has already been classified as starburst (Garcia-Vargas et al. 1990; Kinney et al. 1993), Seyfert 2 (Mouri et al. 1989) and LINER (Díaz 1985; Storchi-Bergmann et al. 1996a). Our nuclear spectrum is consistent with a LINER classification. Its W and colour profiles (Fig. 38) are very similar to those of the previous two galaxies. Both Ws and continuum ratios indicate an S4 template at the nucleus, S7 at the $r = 5$ arcsec ring and S4 outside the ring, decreasing to values typical of an S7 template in the outer regions.

The spatio-spectral variations in NGC 1672 are also seen in Fig. 45(a). The correspondence between Figs 38 and 45(a) is clear. The star-forming ring, with its shallower absorption lines and bluer continuum, is visible in the $r = -8$, $+4$ and $+8$ arcsec extractions plotted in Fig. 45(a). The blueing of the spectra towards the outer regions of the galaxy is also illustrated. The +67-arcsec extraction, in particular, crosses an H II region.

These three examples demonstrate that the method employed in this study is able to detect variations of the stellar populations as a function of distance to the nucleus. Star-forming rings, in particular, leave unambiguous signatures in the W and colour profiles.

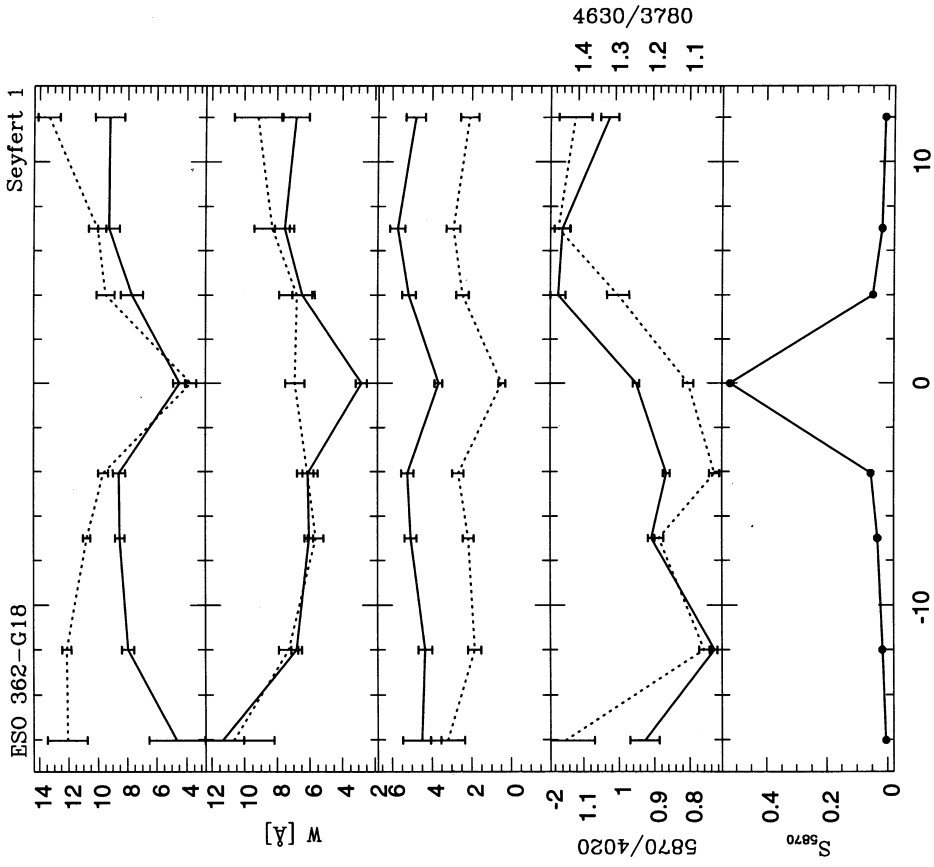

Figure 5. As Fig. 3 but for ESO 362-G18.

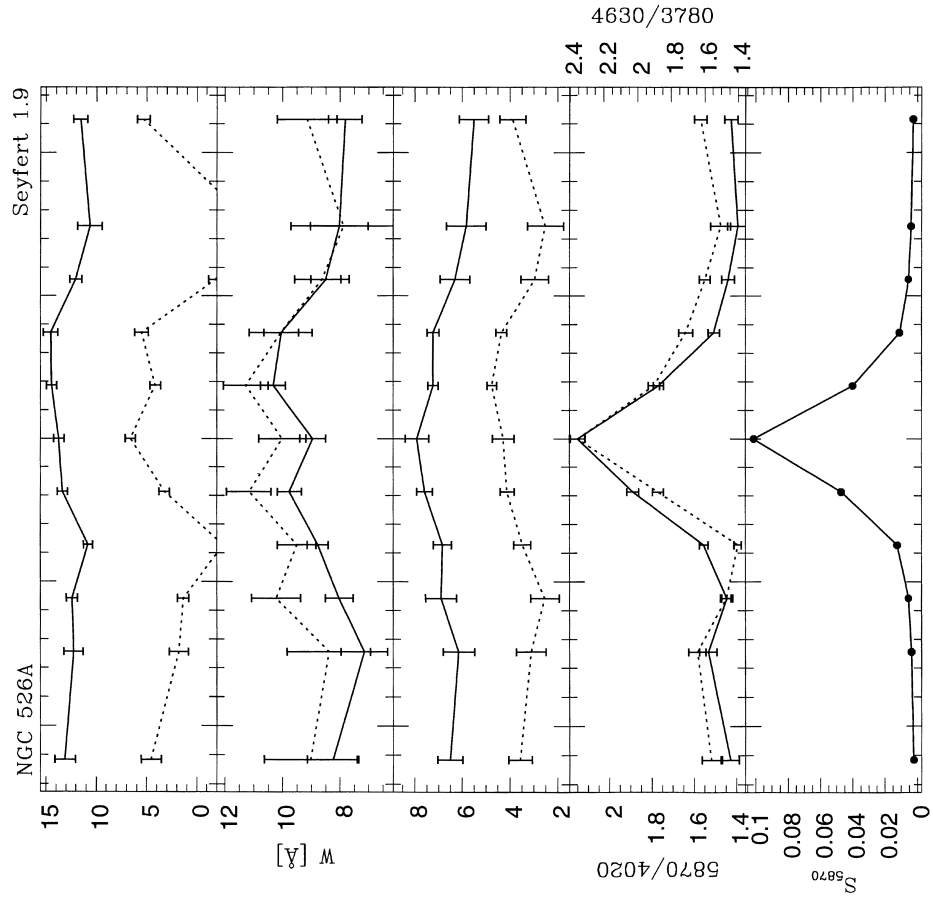

Figure 4. As Fig. 3, but for NGC 526A.

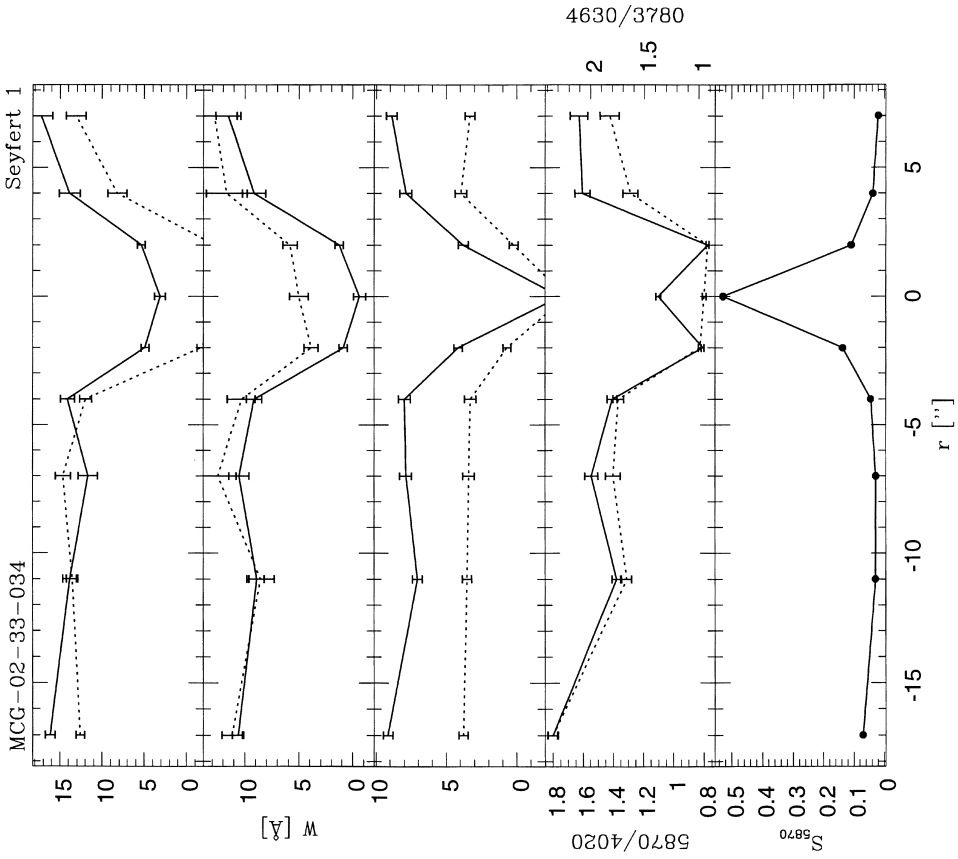

Figure 7. As Fig. 3 but for MCG-02-33-034.

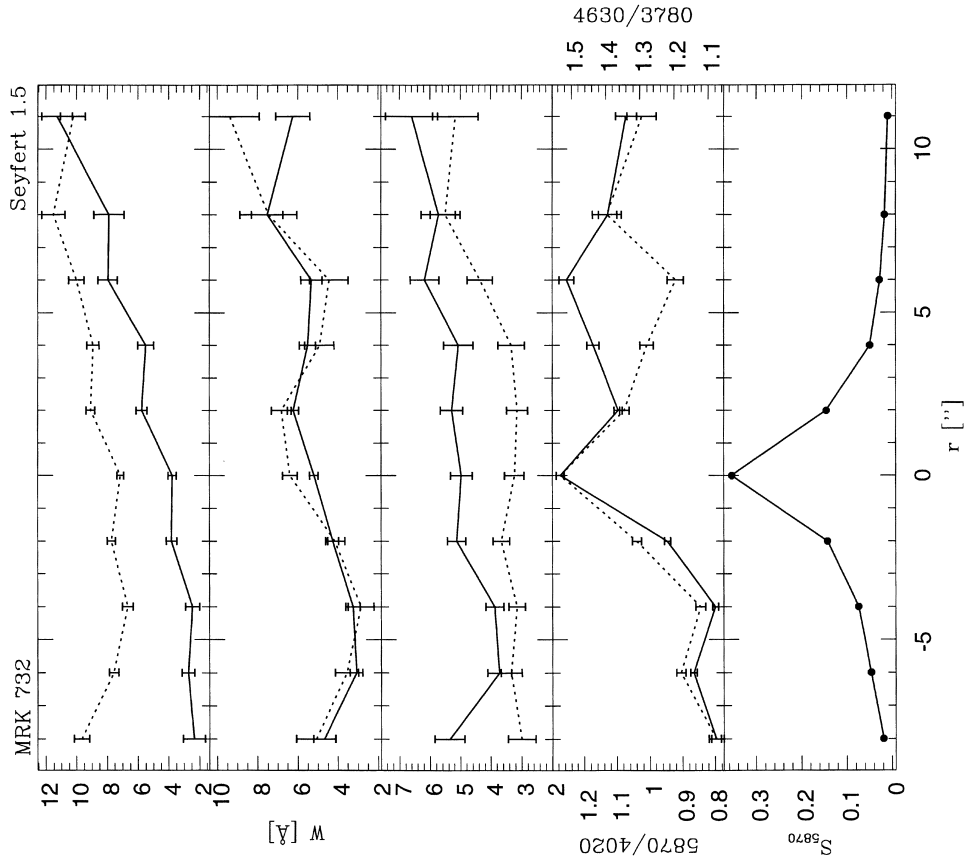

Figure 6. As Fig. 3 but for Mrk 732.

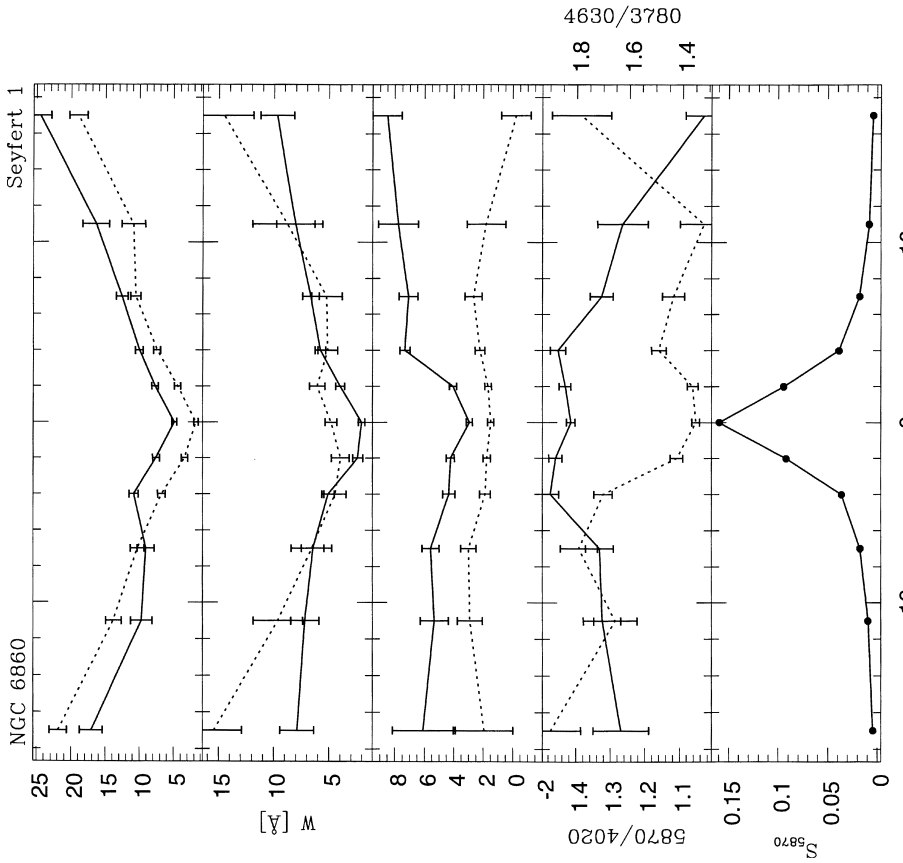

Figure 9. As Fig. 3 but for NGC 6860.

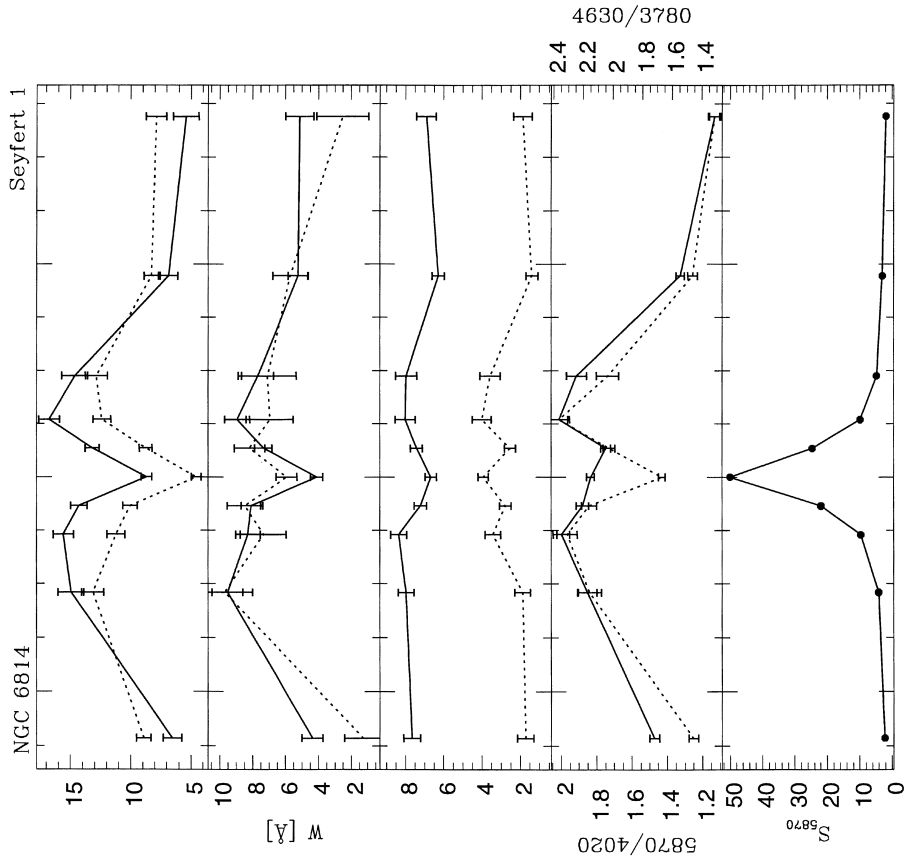

Figure 8. As Fig. 3 but for NGC 6814.

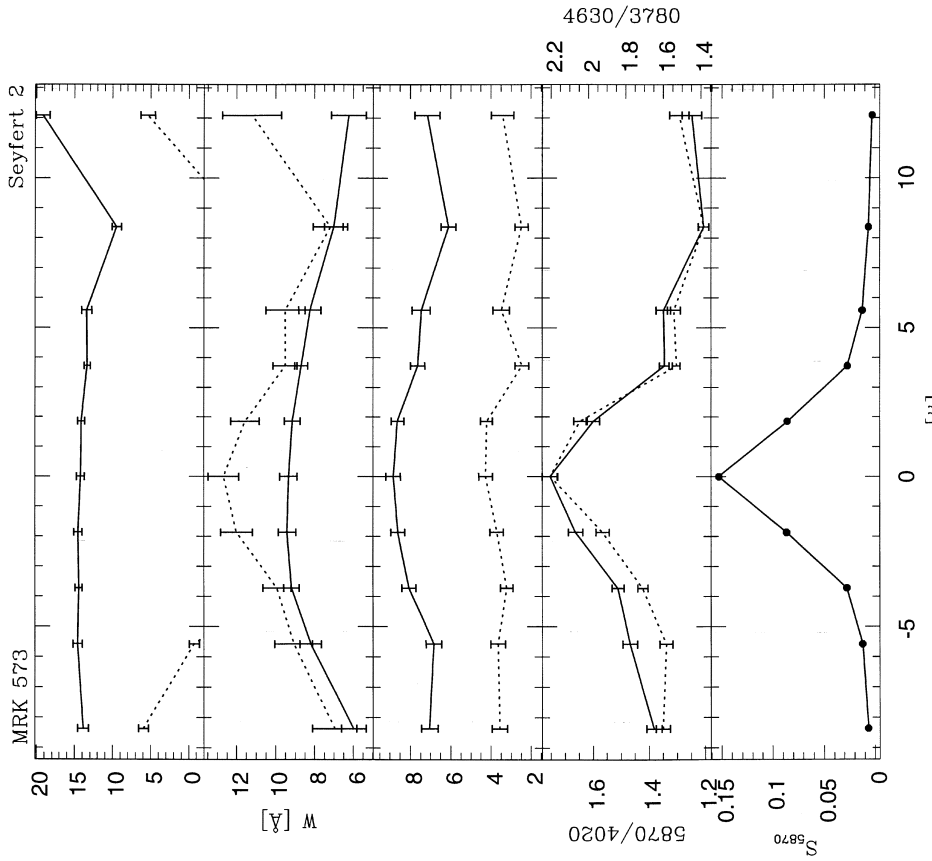

Figure 11. As Fig. 3 but for Mrk 573.

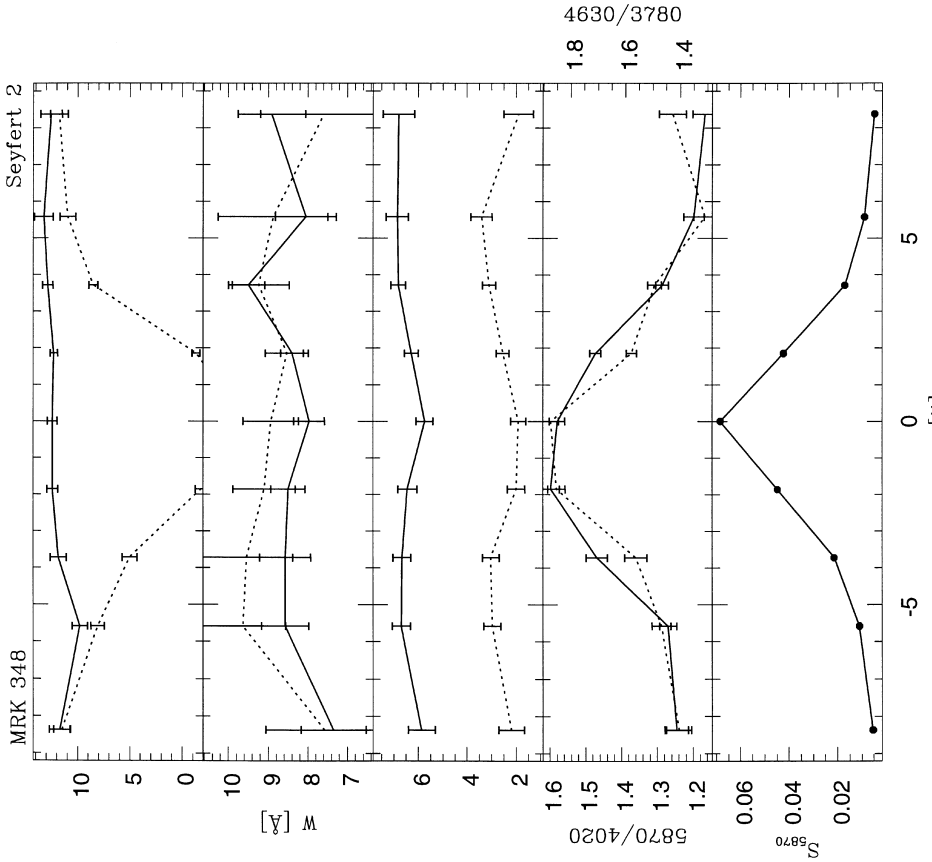

Figure 10. As Fig. 3 but for Mrk 348.

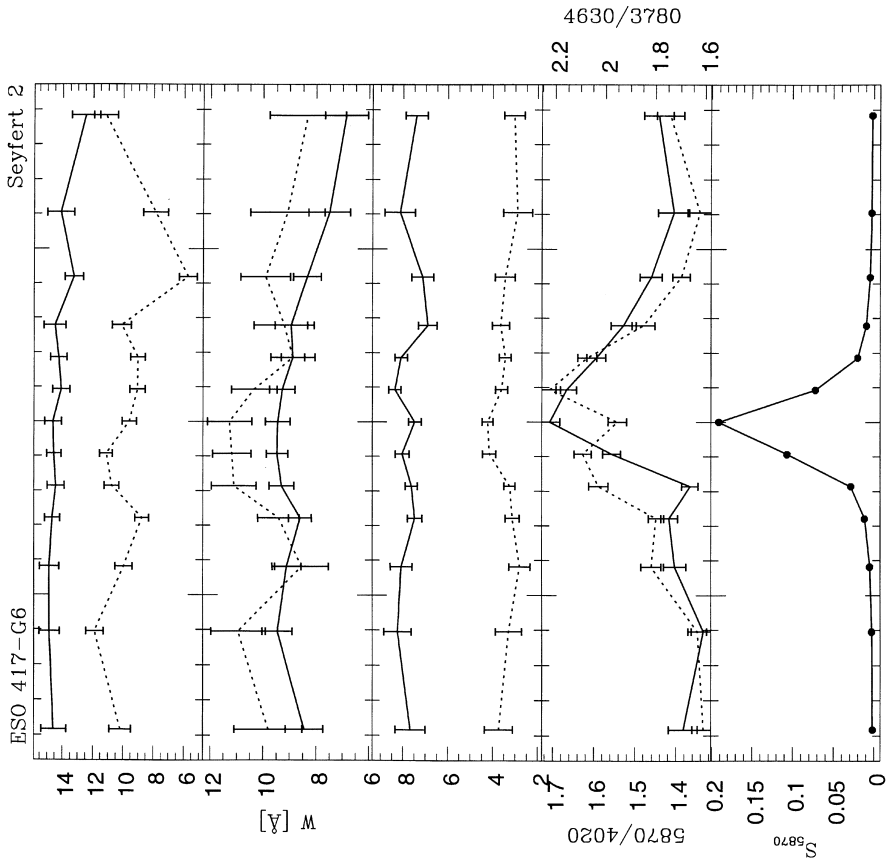

Figure 13. As Fig. 3 but for ESO 417-G6.

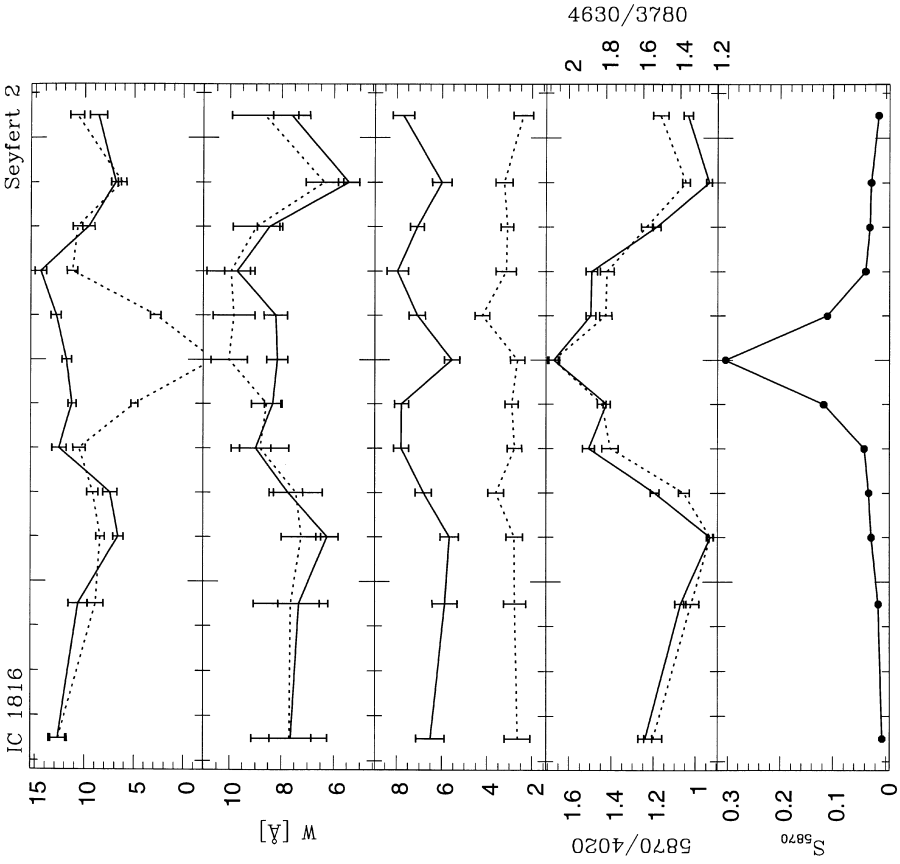

Figure 12. As Fig. 3 but for IC 1816.

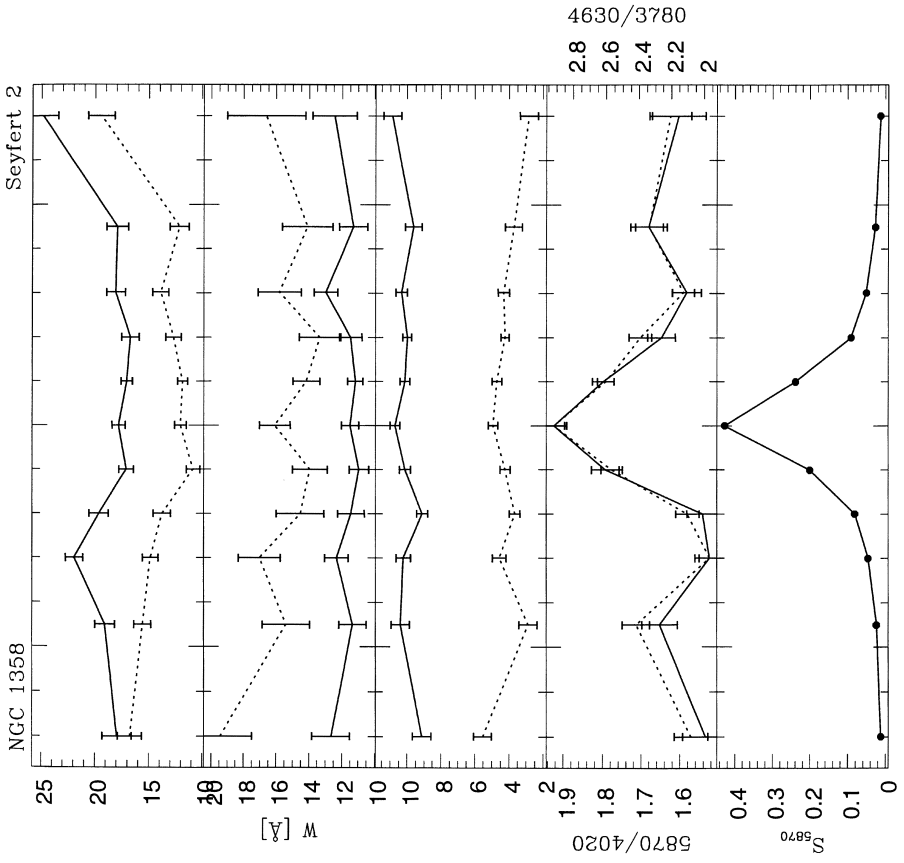

Figure 15. As Fig. 3 but for NGC 1358.

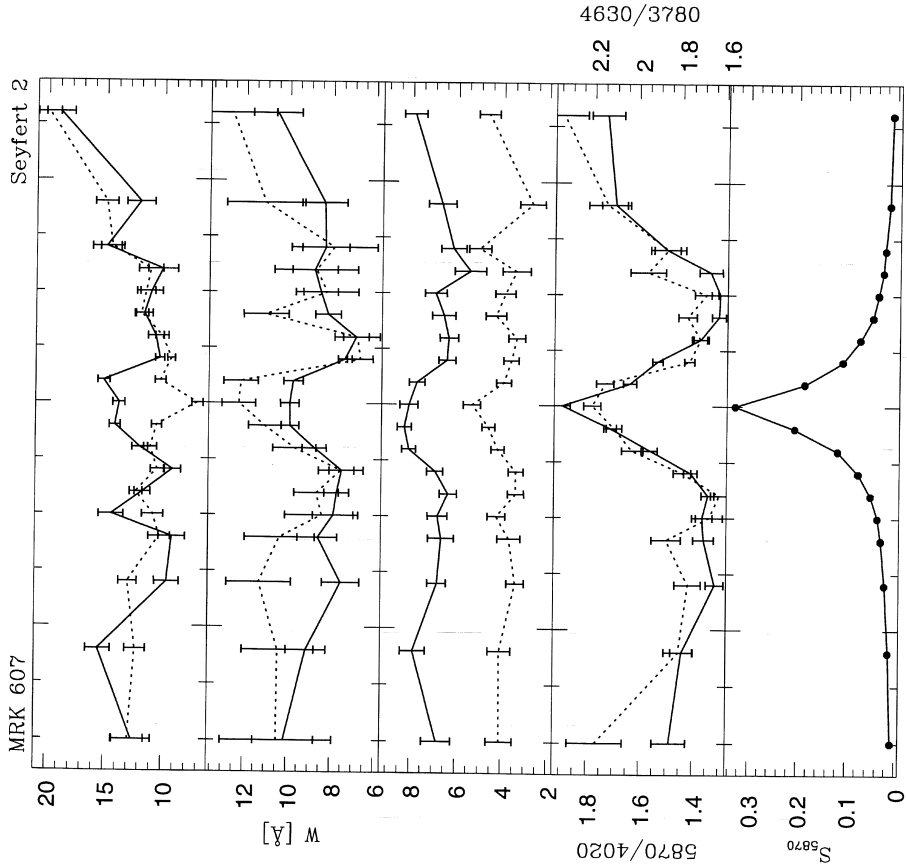

Figure 14. As Fig. 3 but for Mrk 607.

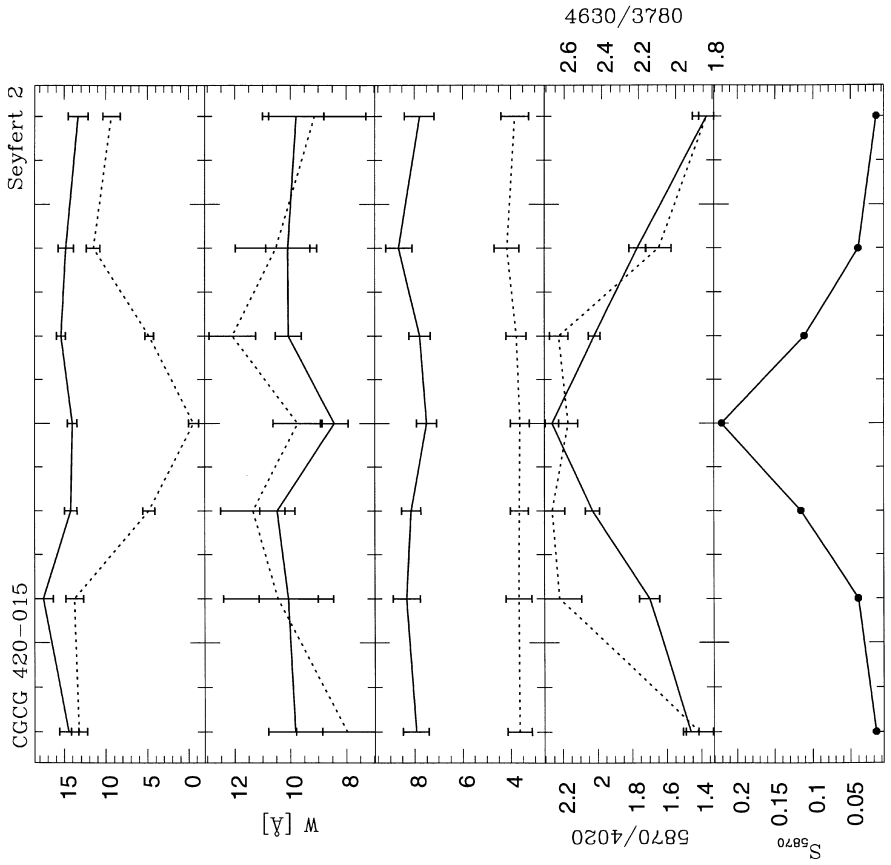

Figure 17. As Fig. 3 but for CGCG 420-015.

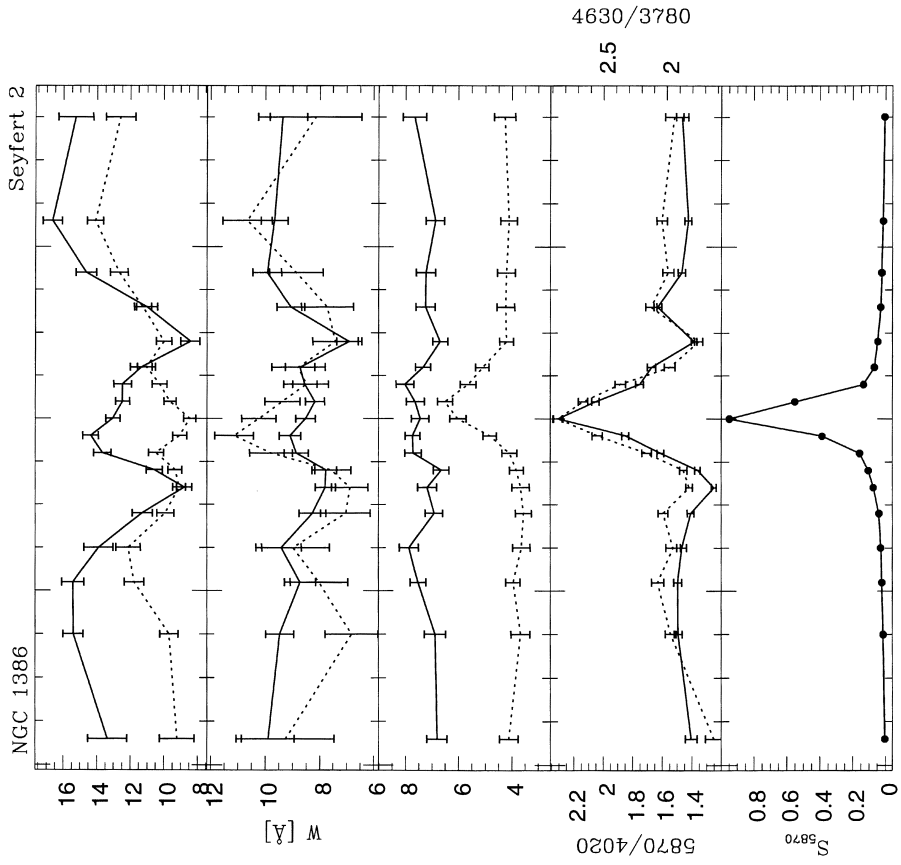

Figure 16. As Fig. 3 but for NGC 1386.

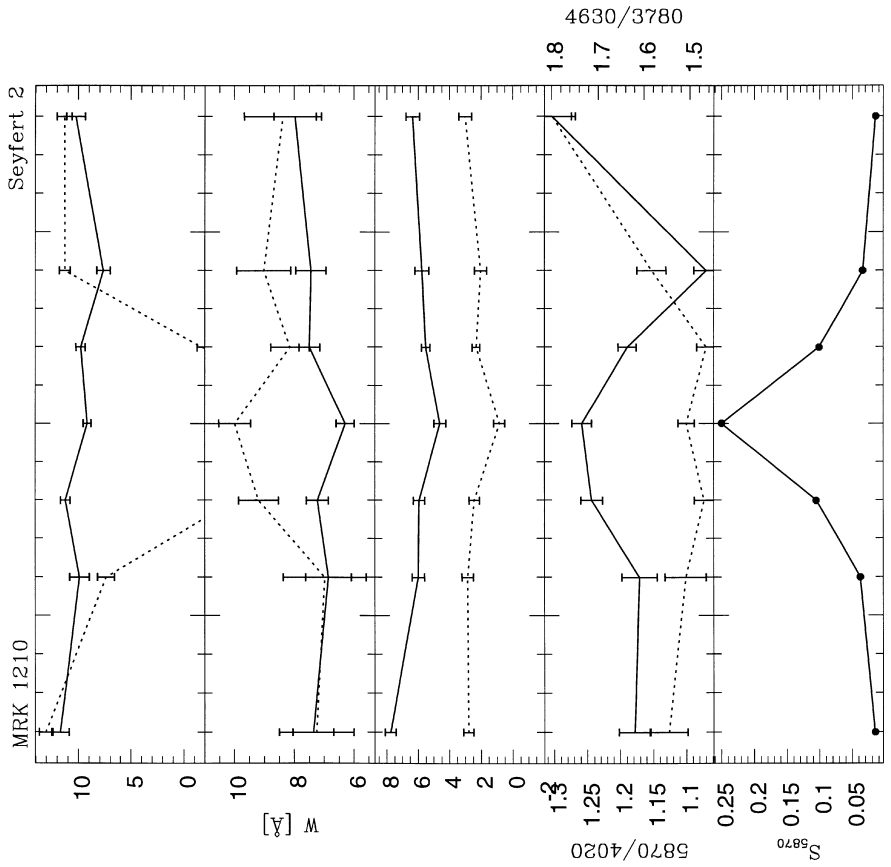

Figure 19. As Fig. 3 but for Mrk 1210.

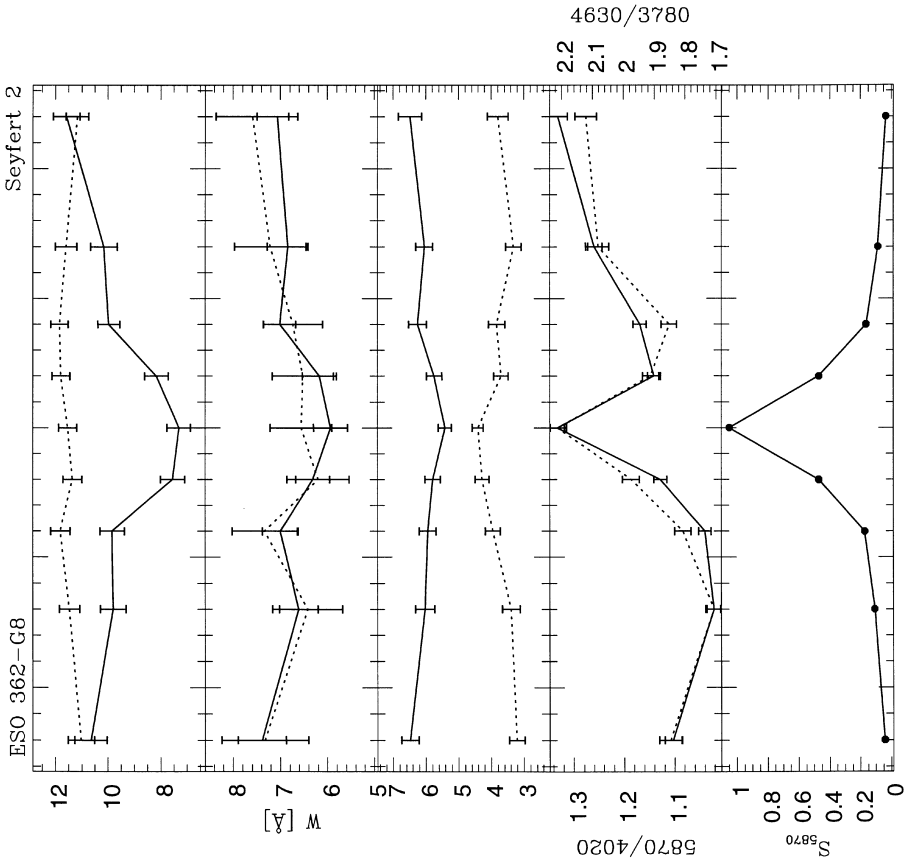

Figure 18. As Fig. 3 but for ESO 362-G8.

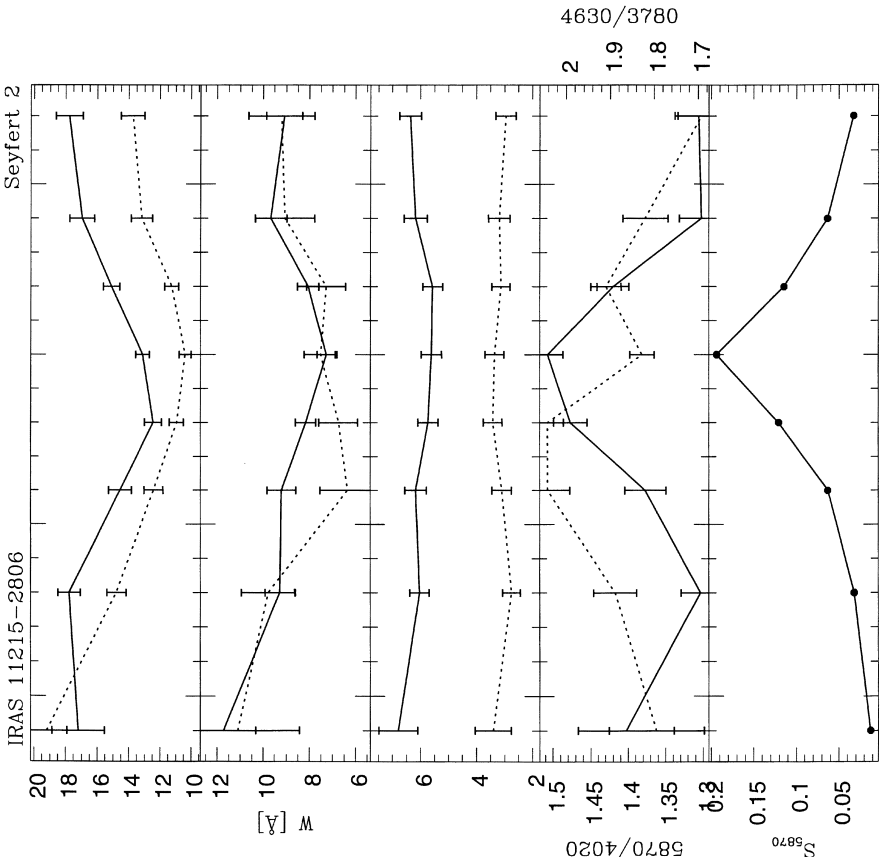

Figure 21. As Fig. 3 but for IRAS 11215−2806.

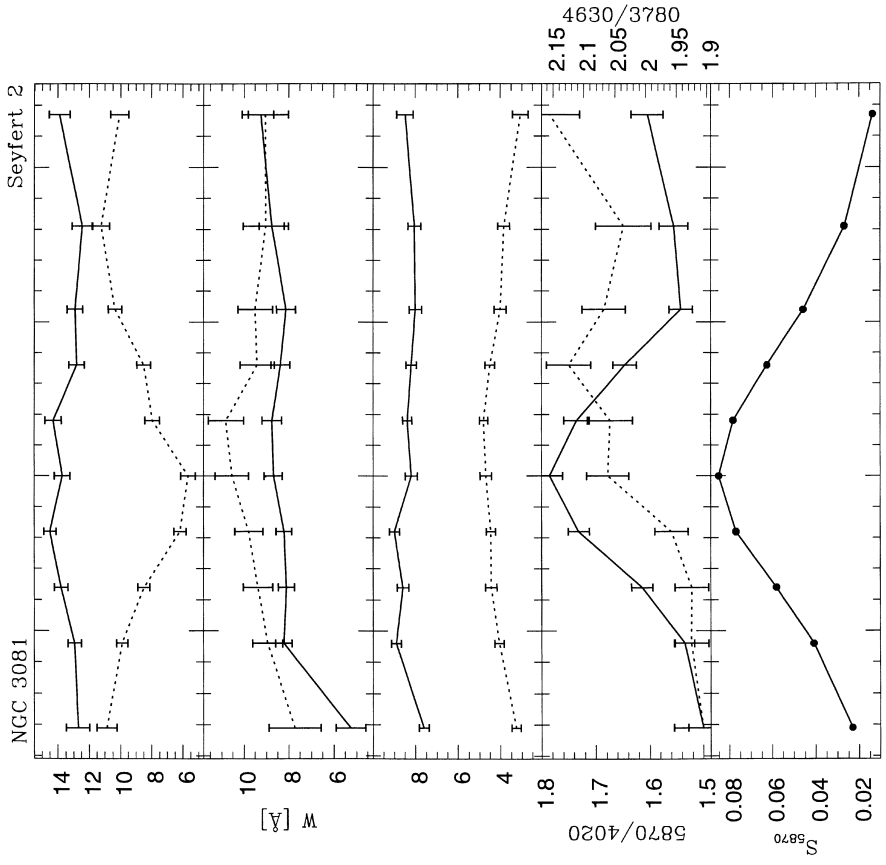

Figure 20. As Fig. 3 but for NGC 3081.

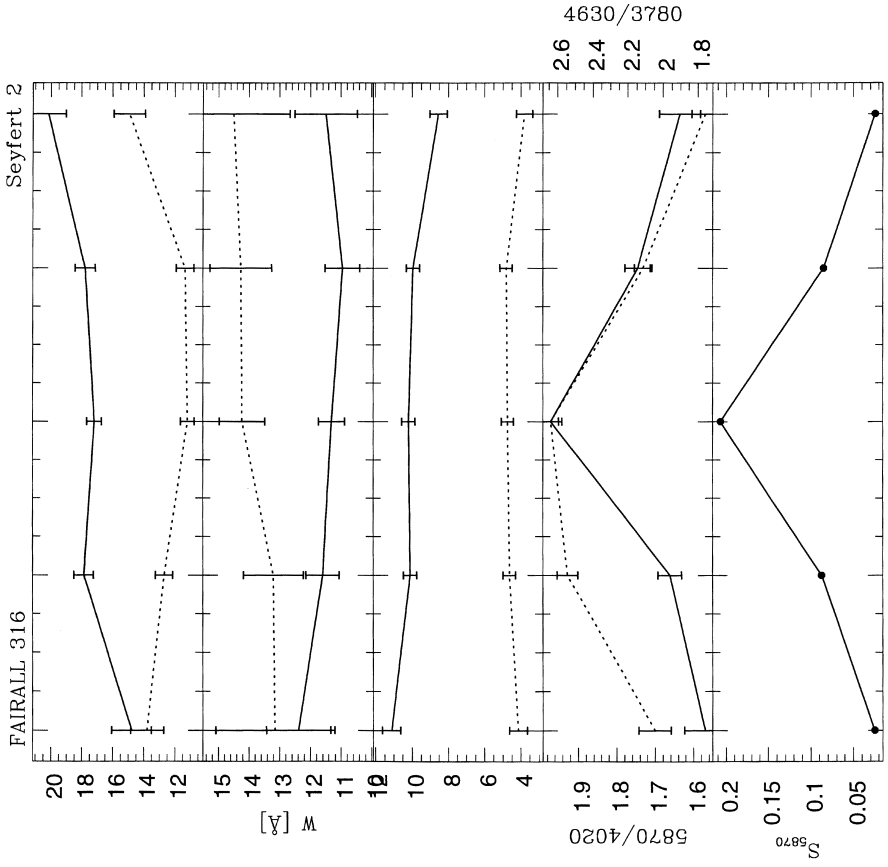

Figure 23. As Fig. 3 but for Fairall 316.

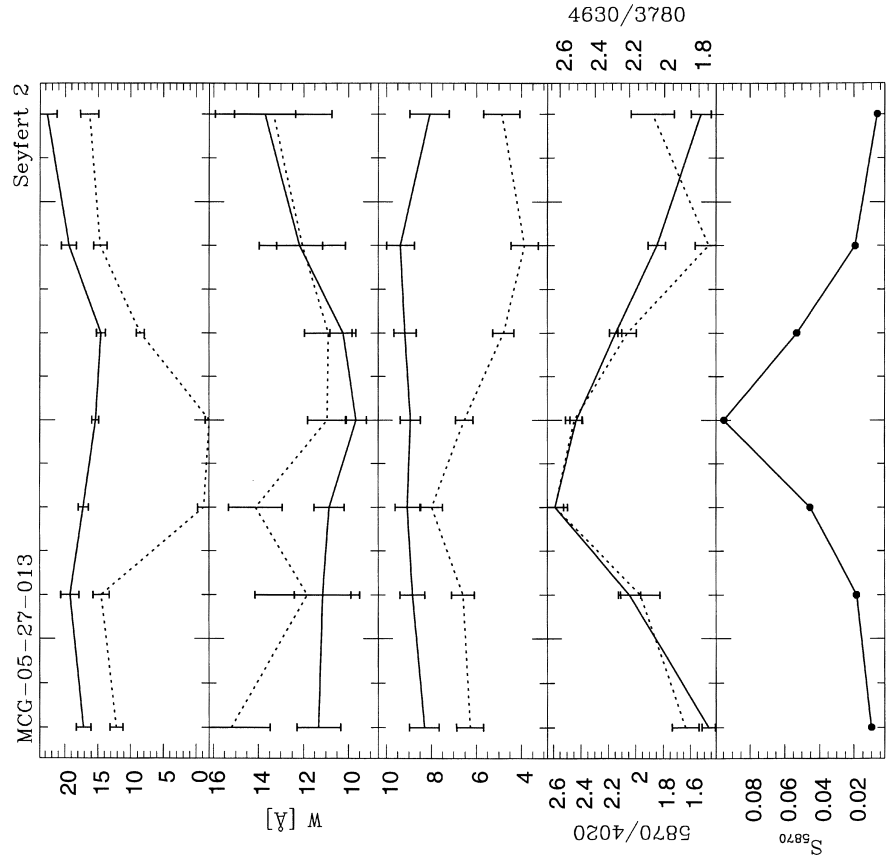

Figure 22. As Fig. 3 but for MCG-05-27-013.

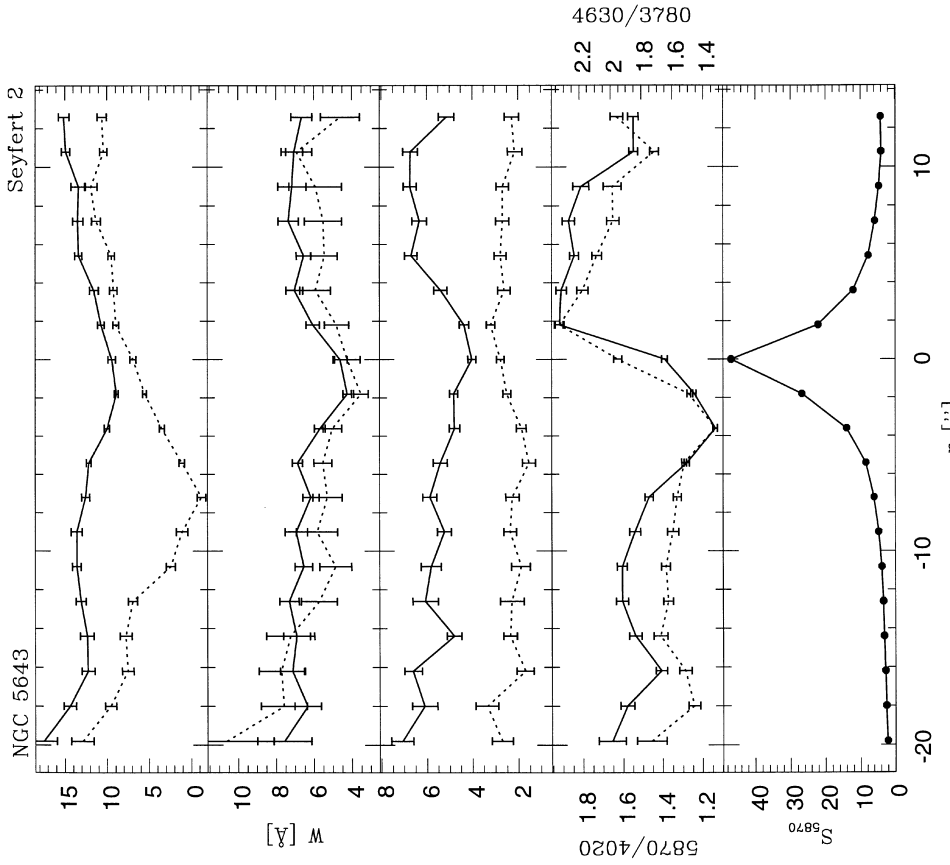

Figure 25. As Fig. 3 but for NGC 5643.

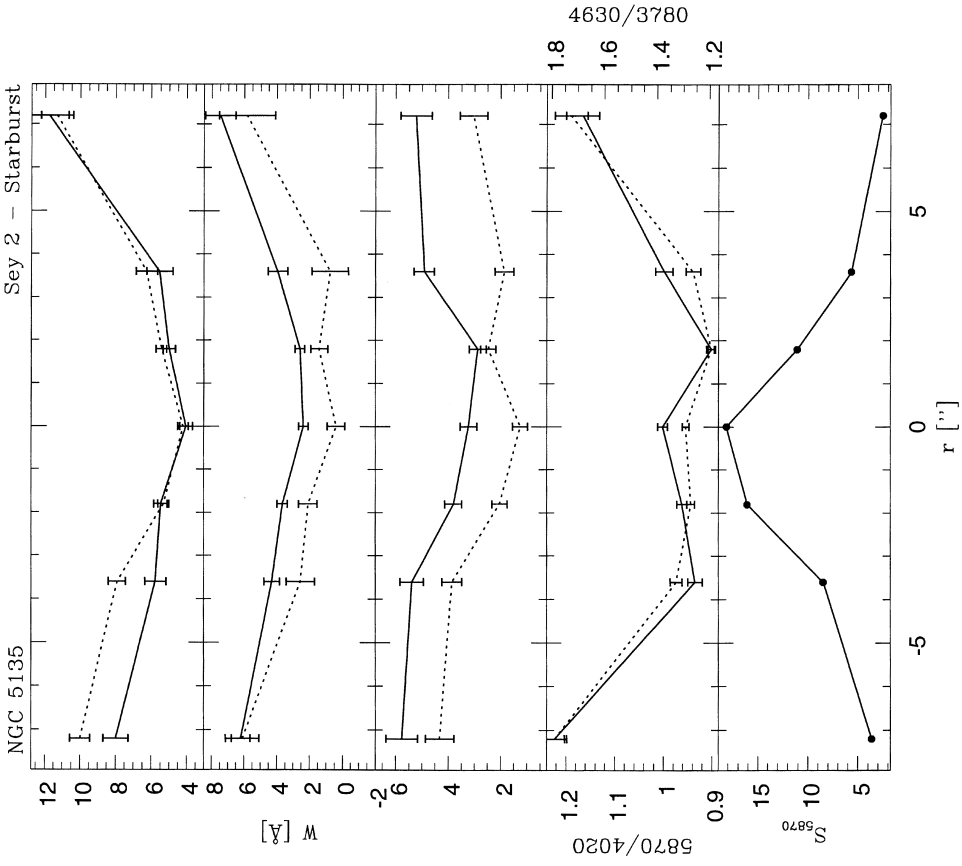

Figure 24. As Fig. 3 but for NGC 5135.

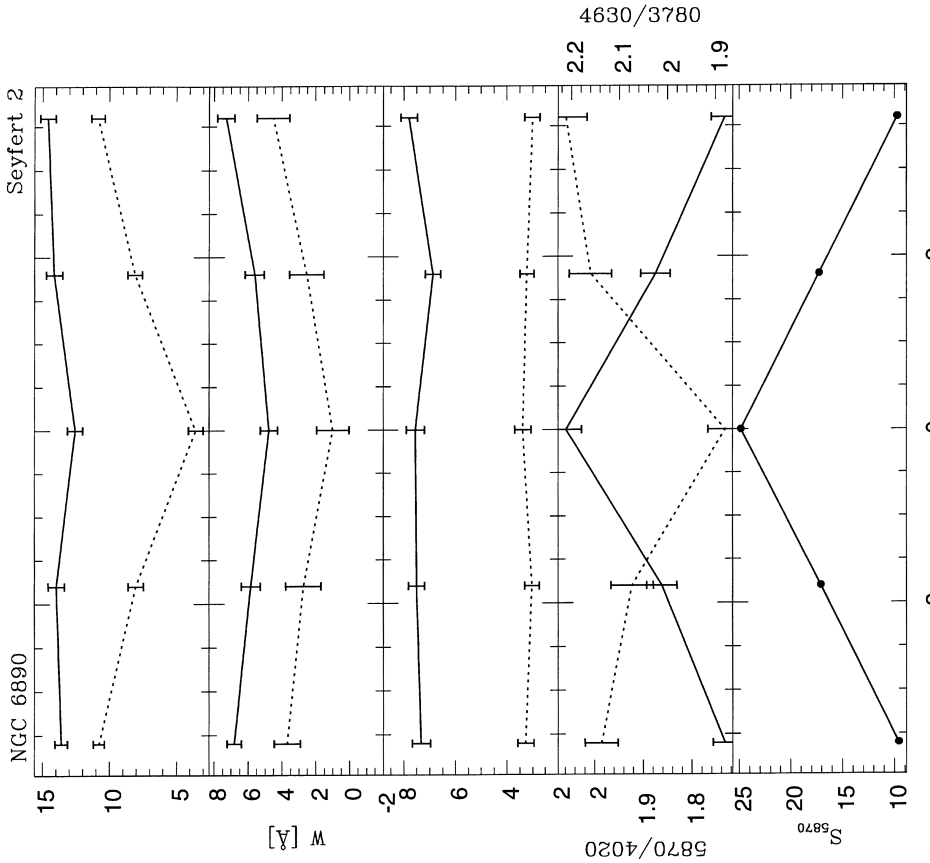

Figure 27. As Fig. 3 but for NGC 6890.

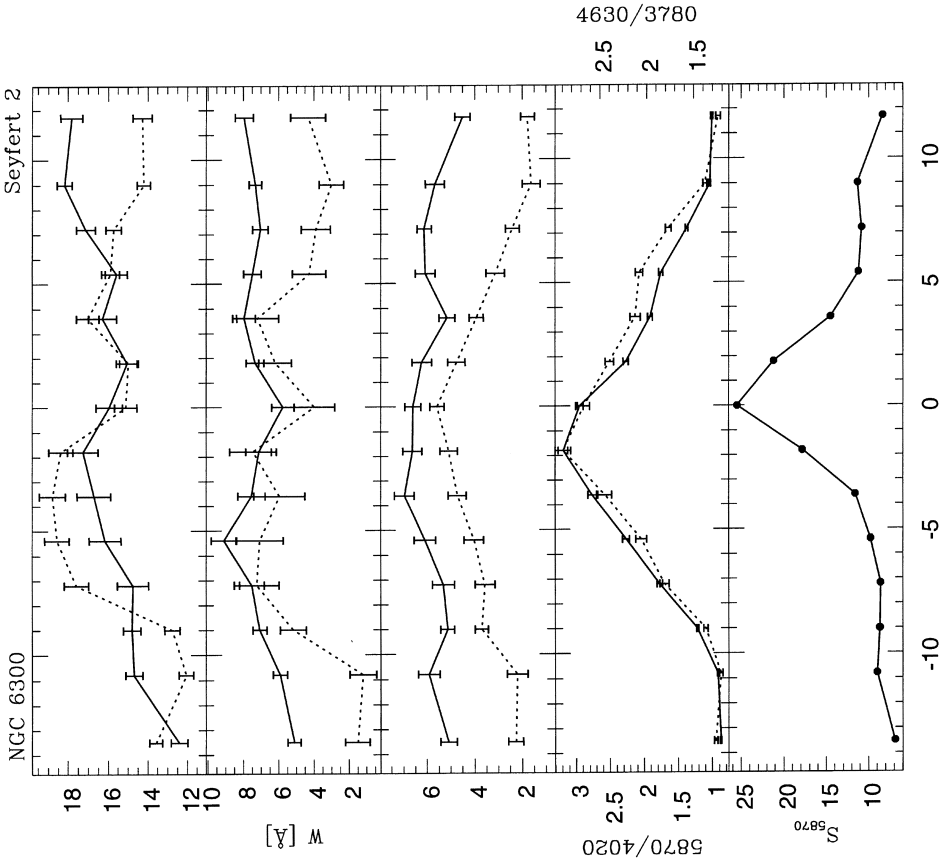

Figure 26. As Fig. 3 but for NGC 6300.

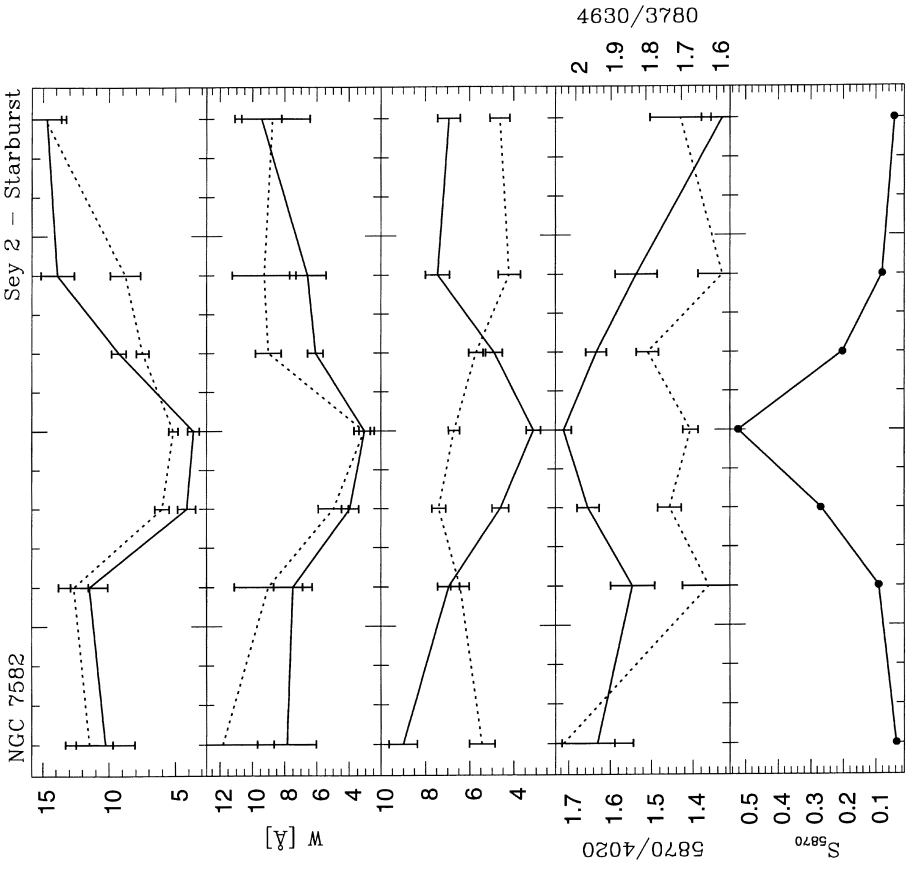

Figure 29. As Fig. 3 but for NGC 7582.

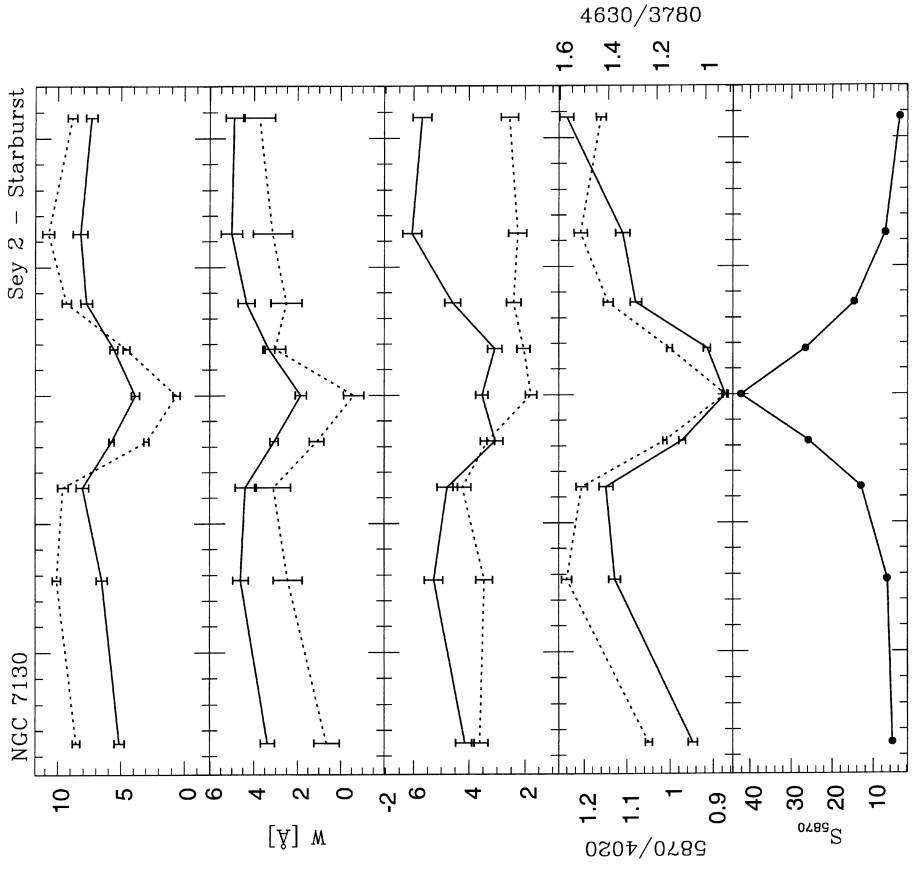

Figure 28. As Fig. 3 but for NGC 7130.

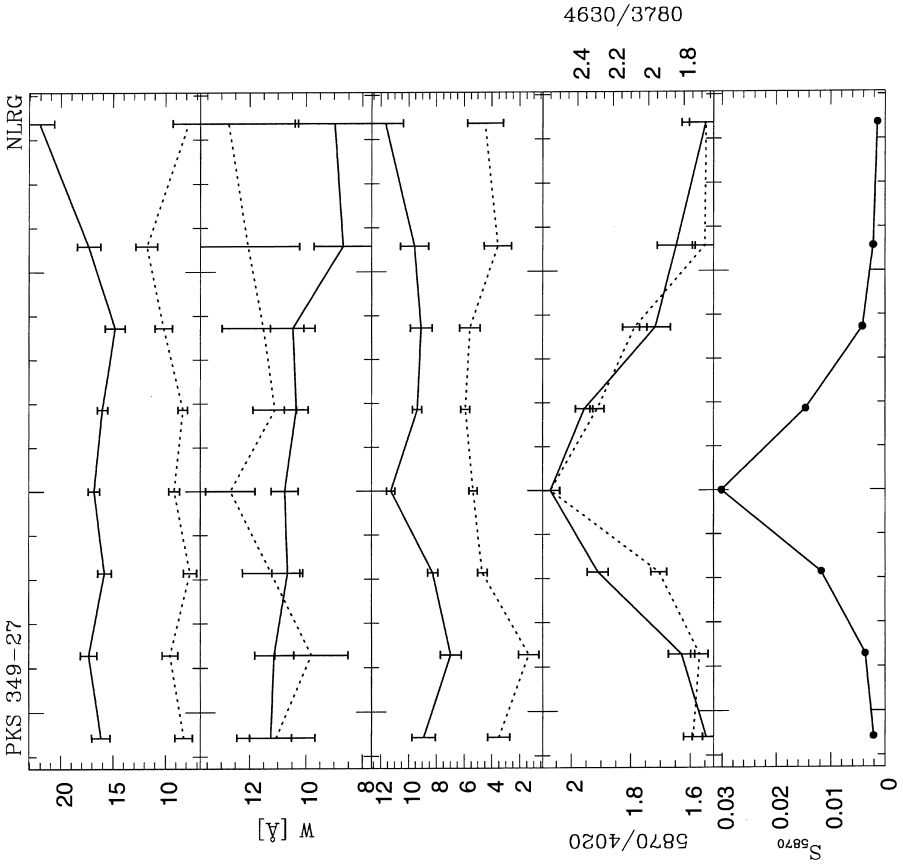

Figure 31. As Fig. 3 but for PKS 349−27.

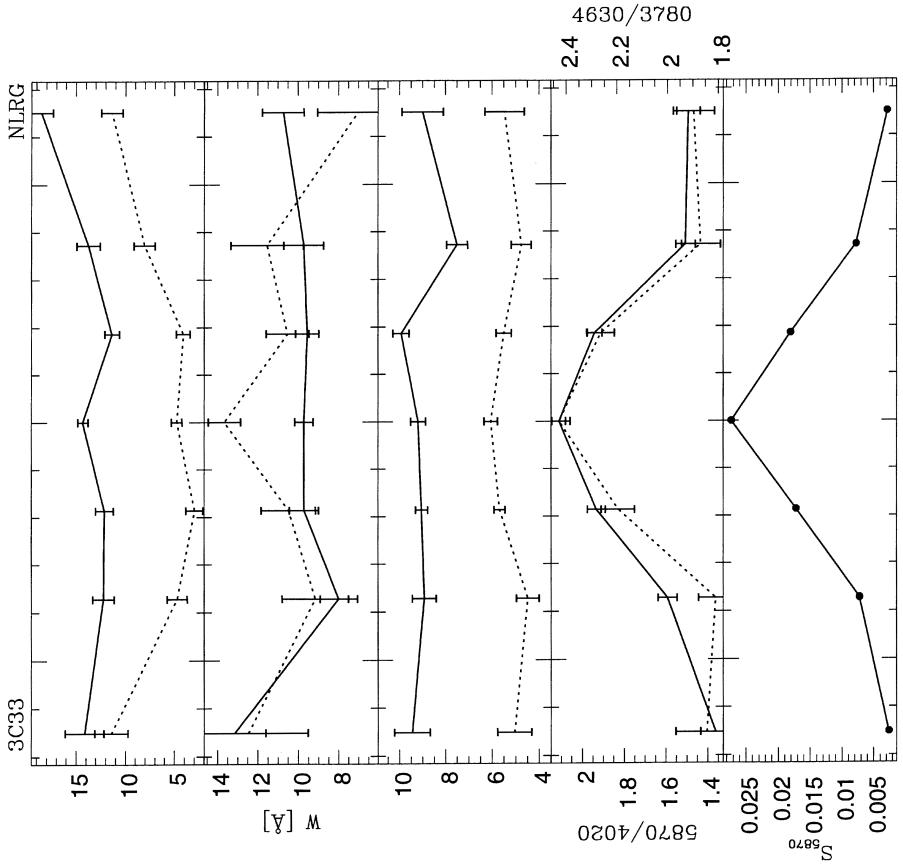

Figure 30. As Fig. 3 but for 3C 33.

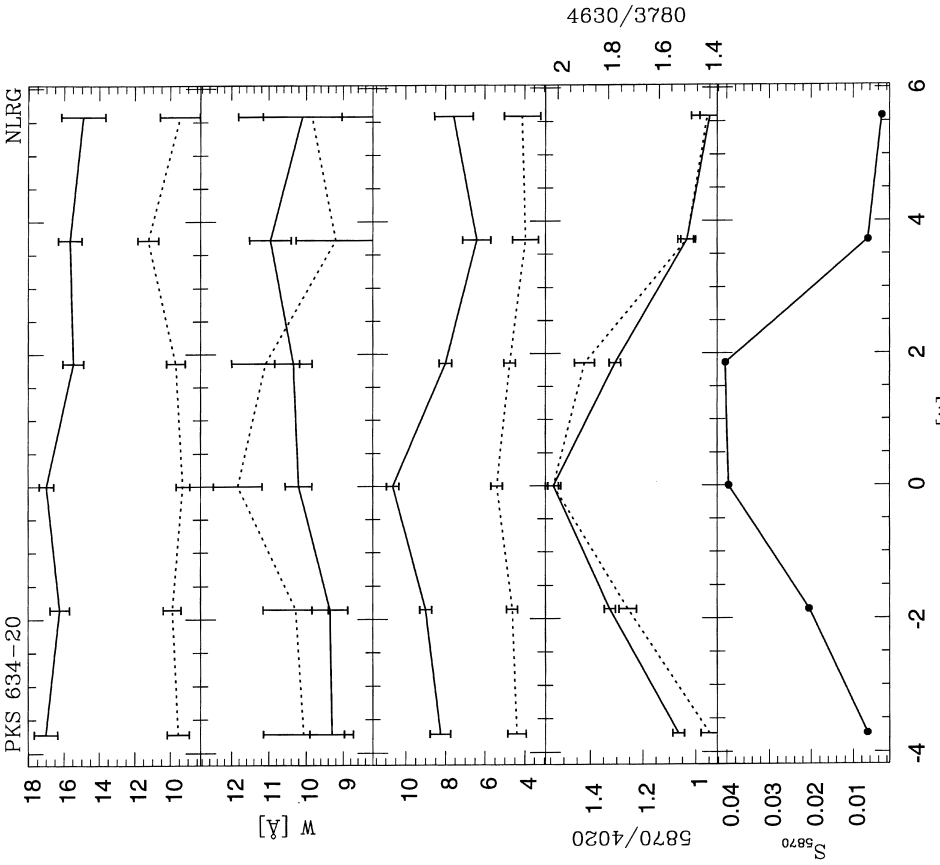

Figure 33. As Fig. 3 but for PKS 634−20.

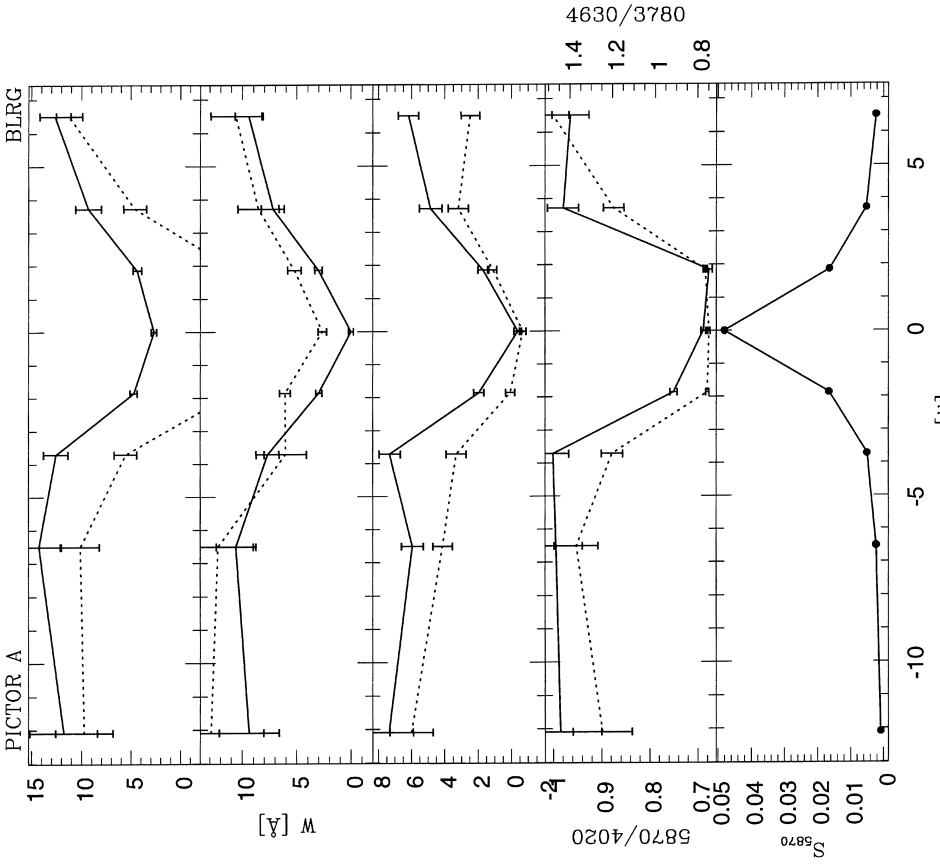

Figure 32. As Fig. 3 but for Pictor A.

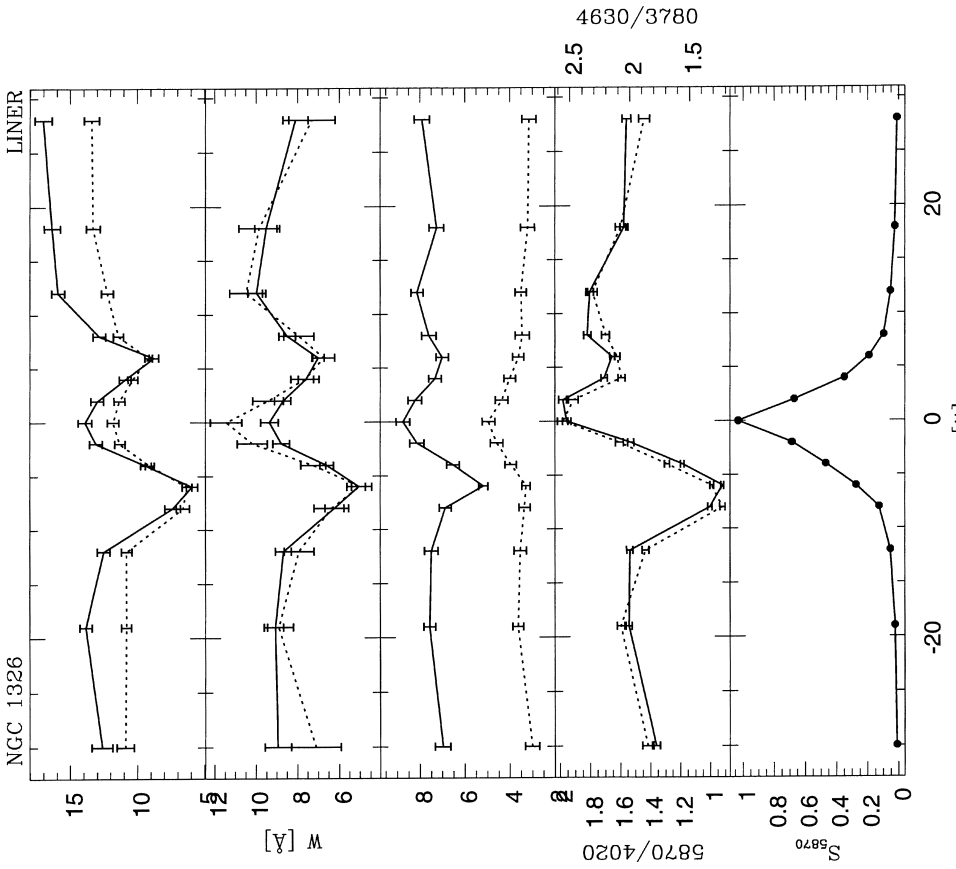

Figure 35. As Fig. 3 but for NGC 1326.

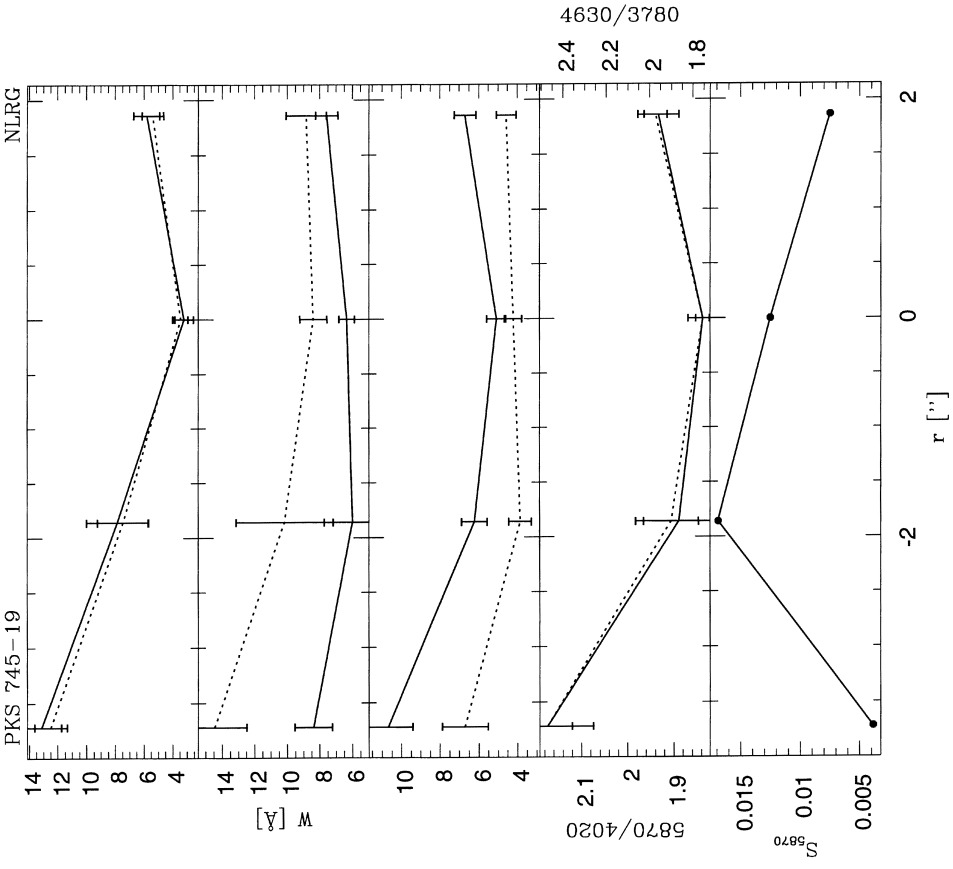

Figure 34. As Fig. 3 but for PKS 745−19.

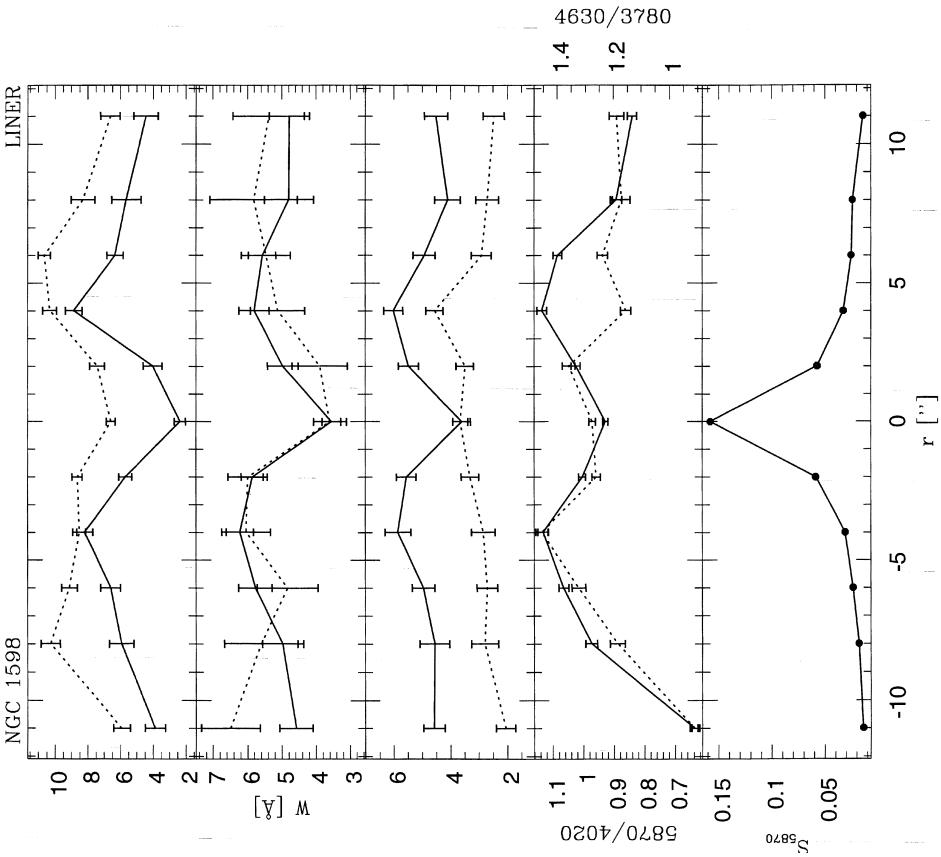

Figure 37. As Fig. 3 but for NGC 1598.

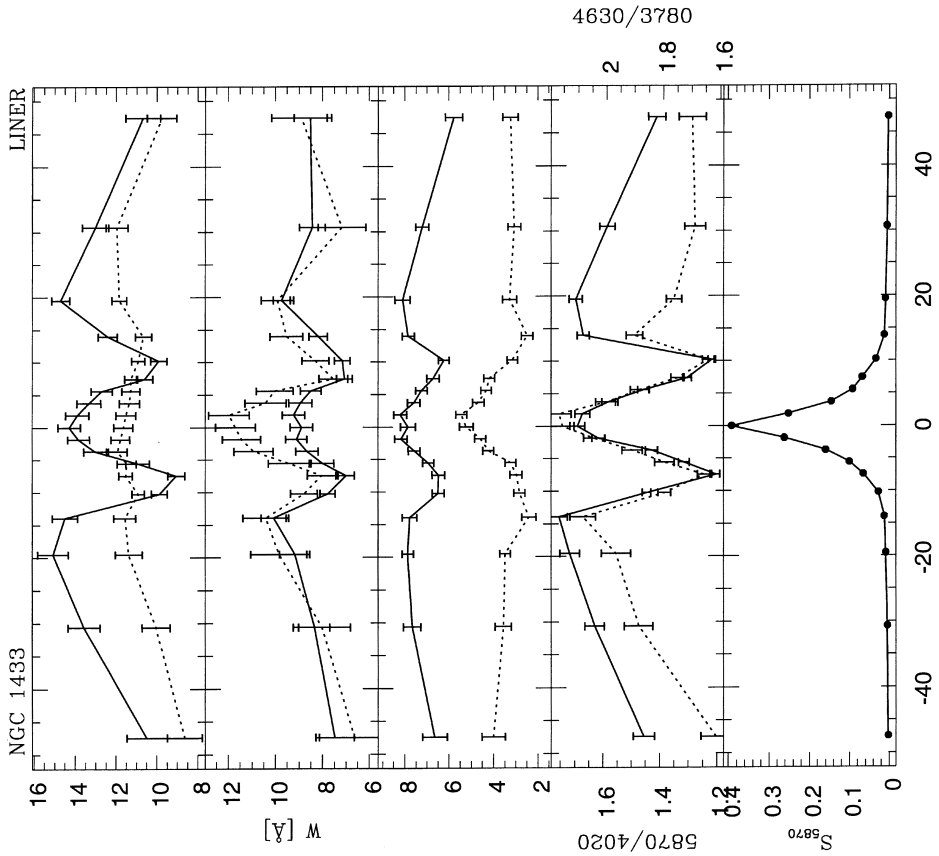

Figure 36. As Fig. 3 but for NGC 1433.

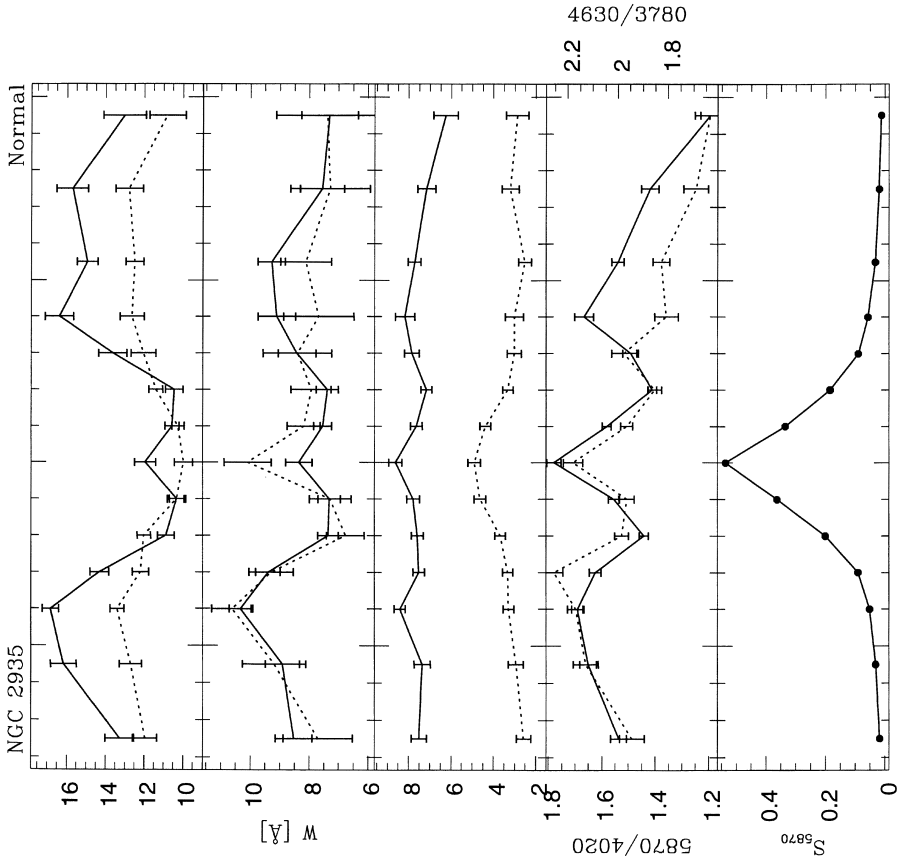

Figure 39. As Fig. 3 but for NGC 2935.

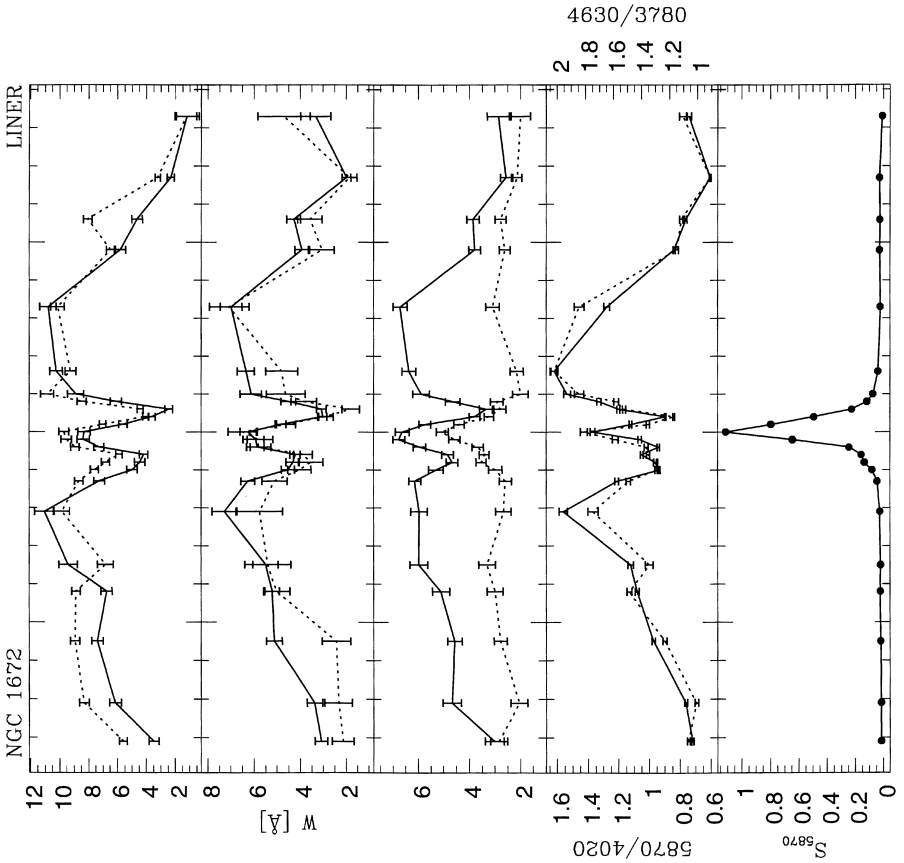

Figure 38. As Fig. 3 but for NGC 1672.

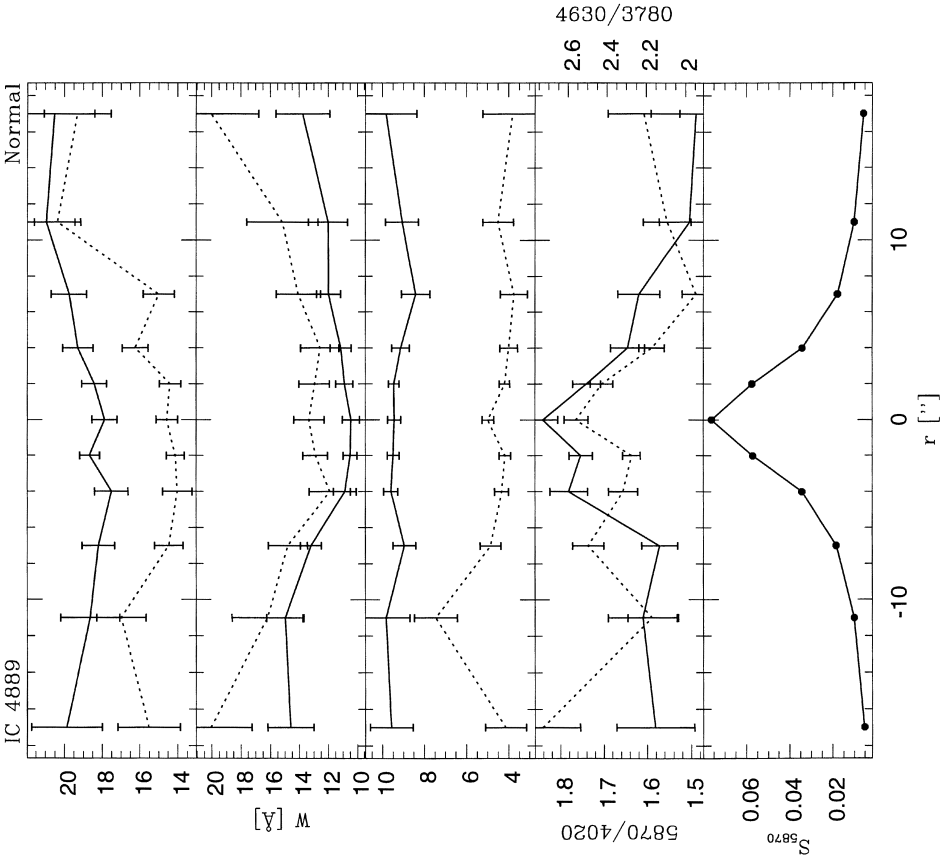

Figure 41. As Fig. 3 but for IC 4889.

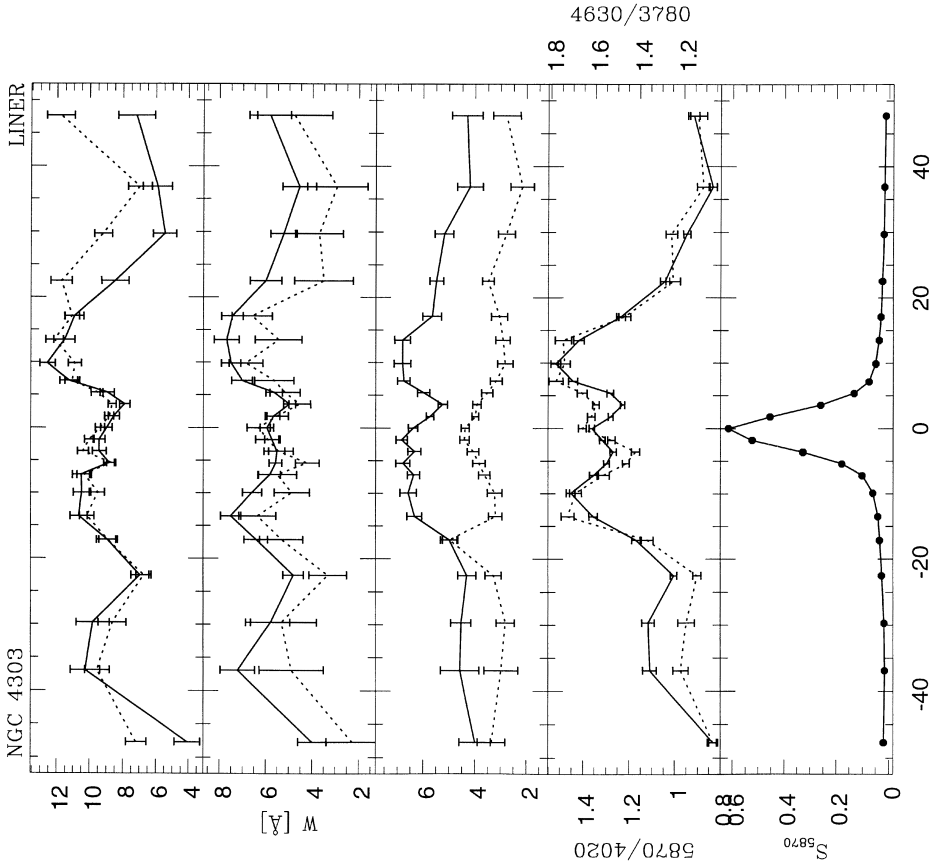

Figure 40. As Fig. 3 but for NGC 4303.

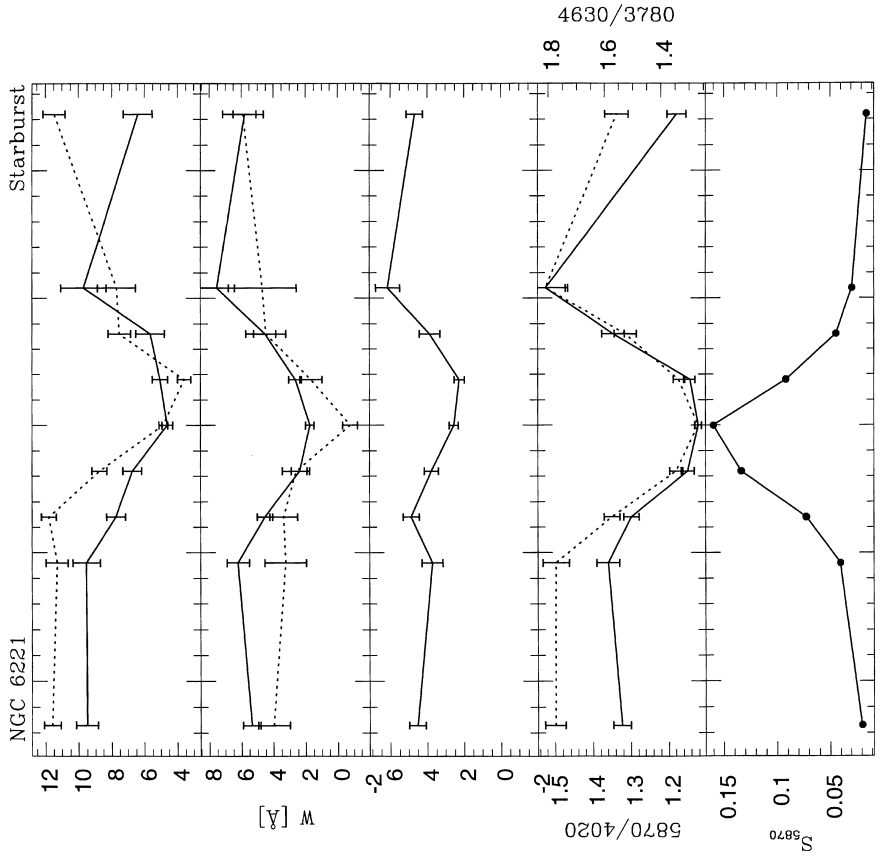

Figure 43. As Fig. 3 but for NGC 6221.

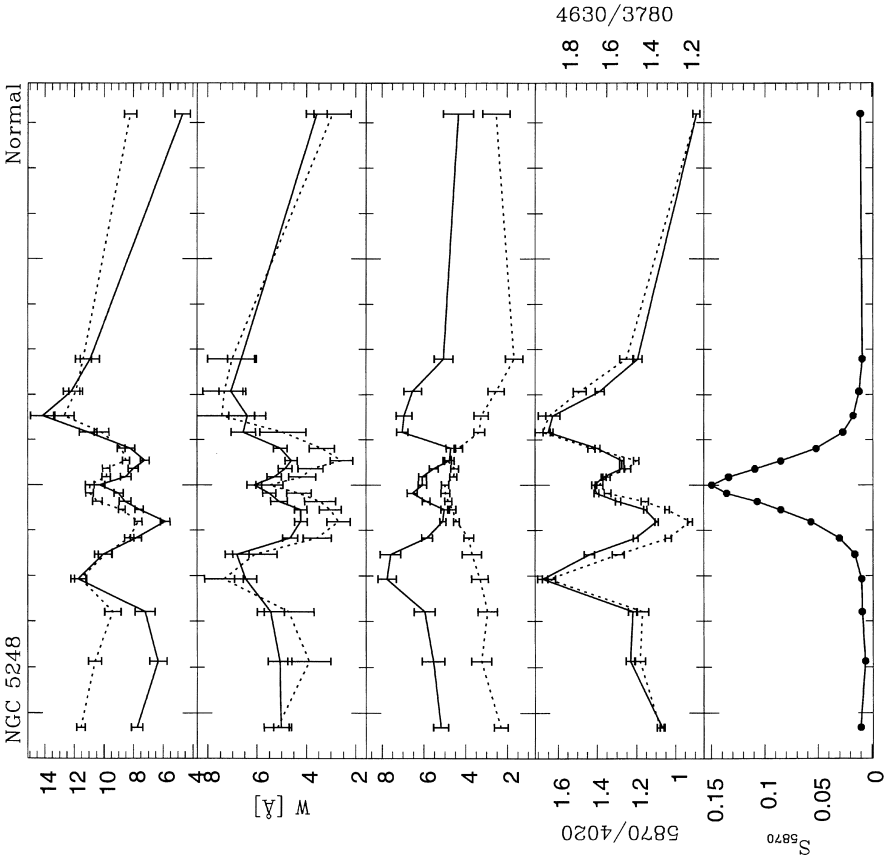

Figure 42. As Fig. 3 but for NGC 5248.

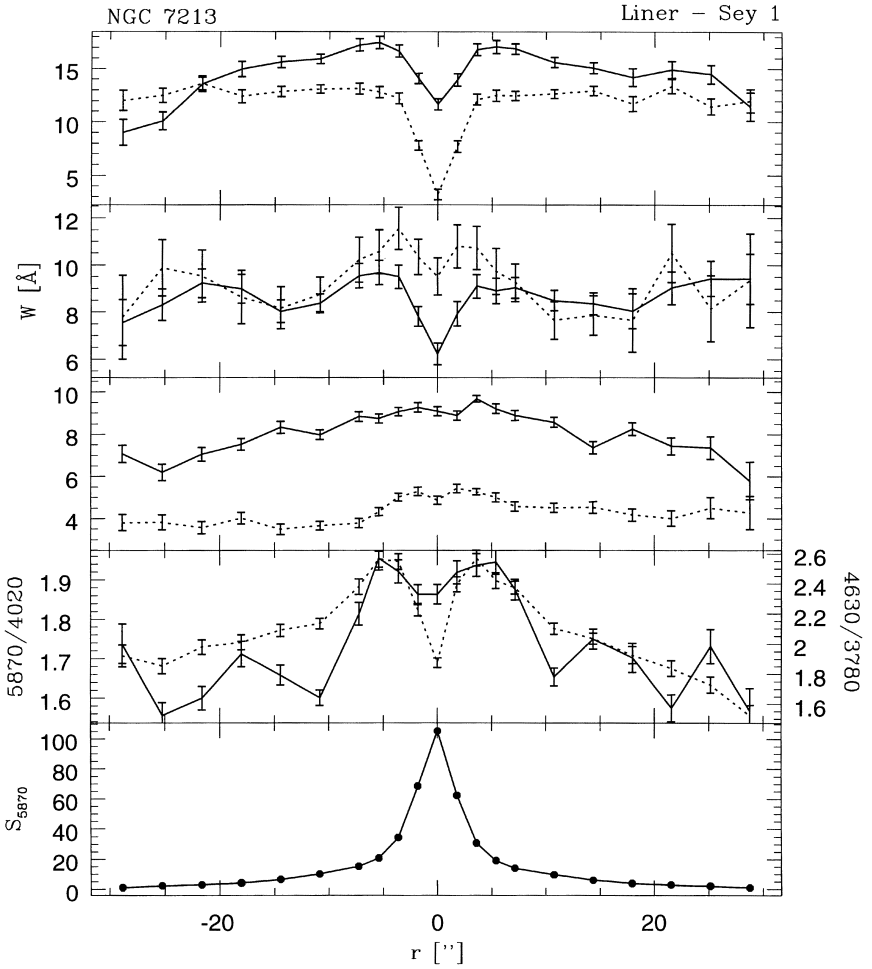

Figure 44. As Fig. 3 but for NGC 7213.

Since 'dilution' of the metal lines by a young stellar population is detectable, we also expect to be able to measure dilution by an AGN continuum. This is best illustrated in the case of Seyfert 1 objects, such as MCG-02-33-034 (Fig. 7), ESO 362-G18 (Fig. 5), NGC 6860 (Fig. 9) and NGC 6814 (Fig. 8), and the broad-line radio galaxy Pictor A (Fig. 32).

One of the clearest examples of dilution by an AGN continuum in our data is NGC 6814 (Figs 8 and 45c). The high degree of variability in both the lines and continuum of NGC 6814 (Yee 1980; Sekiguchi & Menzies 1990) is an unequivocal signature of the presence of an AGN in this galaxy. The presence of an FC is reflected in our W profiles, which show substantial dilution in the nucleus. Comparing the values of the nuclear Ws with those between $|r|$ =5 and 11 arcsec, we obtain dilution factors of 47 per cent for Ca K, 28 per cent for CN, 53 per cent for the G band and 22 per cent for Mg. The larger dilution in the G band is due to broad Hγ entering the line window (Fig. 45c). The FC also affects the nuclear colours, which are bluer than in the neighbouring regions (Fig. 8). The Ws and continuum ratios at 5 arcsec from the nucleus correspond to an S2–S3 template, changing to S5–S6 farther out. The attribution of a spectral template to the nucleus is not meaningful in this case given the obvious presence of a non-stellar continuum.

An interesting case of a galaxy showing signs of dilution is that of the LINER/Seyfert 1 NGC 7213 (Phillips 1979; Filippenko & Halpern 1984). Our W profiles show a clear drop in the Ws of Ca K, CN and the G band, but not in Mg. (Ca H is also diluted, but mostly due to Hϵ.) This indicates that the FC is not strong enough in the 5100-Å region to dilute the Mg line, but its contrast with the stellar component increases towards shorter wavelengths, resulting in a dilution of ~31 per cent of Ca K. This value is very similar to that obtained by Halpern & Filippenko (1984).

Apart from their dilution at the nucleus of NGC 7213, the Ws of Ca K and H, CN and the G band indicate an S2–S3 template at 5 arcsec and farther out. Mg has a W similar to that of an S1 template at the nucleus, gradually changing to S4 in the outer regions. The continuum ratios are similar to an S2 template in the inner 5 arcsec radius, decreasing to S3 farther out. The stellar population template obtained by Bonatto et al. (1989) is S2, similar to the values that we obtained for the regions outside the nucleus.

In Fig. 45(b) we show the spatially resolved, zoomed spectra of NGC 7213. The correspondence between the W variations in Fig. 44 and the features in the individual spectra is clearly seen. The dilution of Ca K and H, CN and the G band is observed as shallower absorption lines in the nuclear spectrum, while the lack of dilution in Mg can be seen via the similar depths of the line in different extractions.

4.1 Individual objects

The five cases discussed above fully illustrate the potential of long-slit spectroscopy as a tool to probe stellar population gradients and

the presence of a featureless AGN-like continuum. In this section we provide a description of our results for the remaining objects in our sample, separated by activity class (Seyfert 1s, Seyfert 2s, radio galaxies, LINERs and normal galaxies).

4.1.1 Seyfert 1s

NGC 526a. This is the brightest galaxy of a strongly interacting pair, which presents an optical emission-line region elongated in the direction of the companion galaxy (north-west–south-east: Mulchaey, Wilson & Tsvetanov 1996). Both Ws and continuum ratios of this galaxy present a mild gradient (Fig. 4), but opposite to that expected from dilution by a blue continuum. The Ws are larger at the nucleus, indicating S3–S4 templates, decreasing outwards, with values of S4–S5 templates at 7 arcsec from the nucleus. The continuum ratios indicate the same templates outside the nucleus but a redder ratio at the nucleus, corresponding to an S1 template.

ESO 362-G18. According to Mulchaey et al. (1996), this Seyfert 1 is a strongly perturbed galaxy, with the strongest [O III] emission concentrated in the nucleus and showing an extension to the south-east, suggestive of a conical morphology. The Ws and continuum ratios show a strong dilution by an FC in the nuclear region (Fig. 5). At 5 arcsec and farther out, both Ws and continuum ratios indicate an S5 template.

Mrk 732. The individual spectra (Fig. 1) show signatures of young stars to the north-east of the nucleus ($r < 0$), where the Ws consistently indicate an S7 template. The nuclear Ws indicate a dilution when compared with the wouth-western side ($r > 0$), which shows Ws of an S5 template (Fig. 6). The continuum ratios indicate the same templates.

MCG-02-33-034. This galaxy was classified as Seyfert 1 by Osterbrock & De Robertis (1985), based on the appearence of permitted lines broader than the forbidden ones and strong Fe II emission. Mulchaey et al. (1996) show that it presents evidence of two nuclei, both emitting in [O III] and Hα. We can see the dilution of Ws and colour changes due to a blue FC in the nuclear region (Fig. 7). The Ws change to values of an S3 template at 4 arcsec and farther out, while the continuum ratios have values similar to an S4 at 4 arcsec and farther out. As noted in Section 3, although dilution clearly occurs, the complex nuclear spectrum (Fig. 2d) prevents an accurate determination of both Ws and continuum at $r = 0$ for this galaxy.

NGC 6860. According to Lípari, Tsvetanov & Macchetto (1993) the Hα image of this galaxy shows bright emission-line regions associated with the nucleus and a circumnuclear ring of star formation. The emission-line spectrum is typical of a Seyfert 1.5 and variable. The Ws (Fig. 9) are diluted by an FC at the nucleus. Their values change to those of an S2 template at 4 arcsec and farther out. The continuum ratios show a gradient in the opposite direction, decreasing from S4 in the inner 5 arcsec radius to S5 farther out, bluer than the values indicated by the Ws in the outer regions.

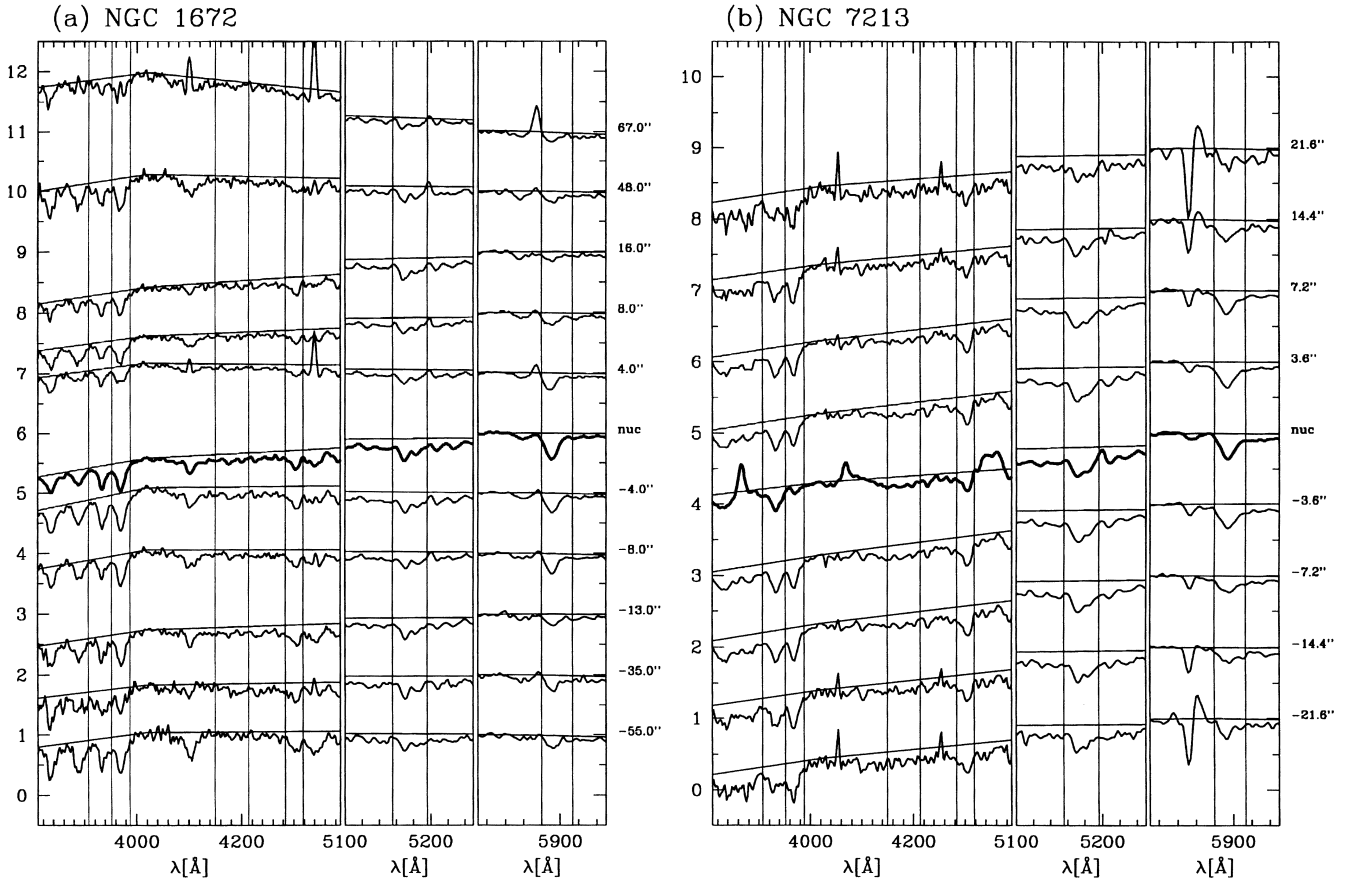

Figure 45. Spectra of five of the sample galaxies for several positions along the slit, zoomed into the regions of the absorption features discussed in this work. (a) NGC 1672, (b) NGC 7213 (c) NGC 6814, (d) Mrk 573 and (e) 3C33. The radial positions are indicated on the right side of the plots.

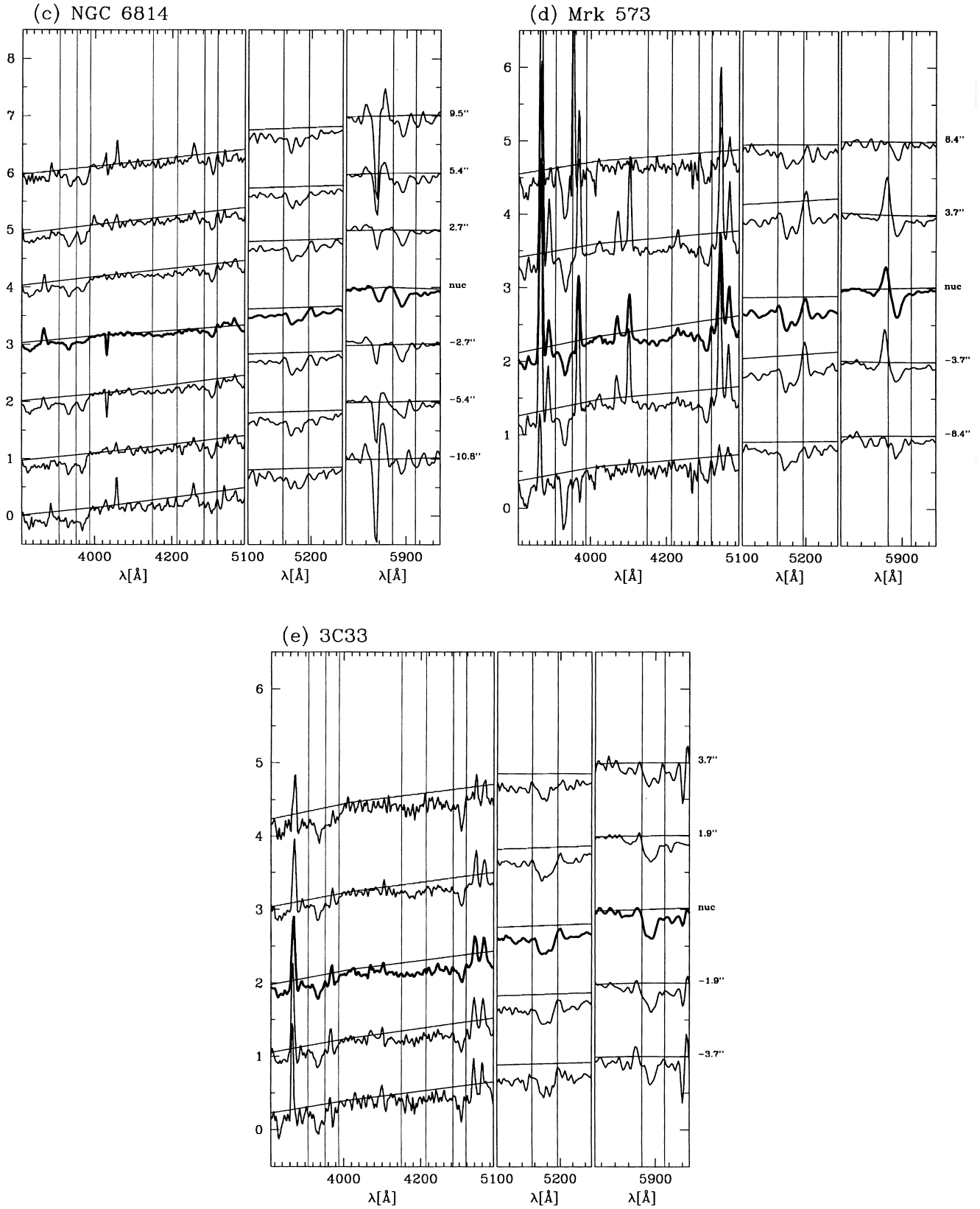

Figure 45 – *continued*

4.1.2 Seyfert 2s

Mrk 348. This is a Seyfert 2 galaxy with evidence of broad Hα (De Robertis & Osterbrock 1986b), He I 10 830-Å and Paβ lines (Ruiz, Rieke & Schmidt 1994). Koski (1978) observed this galaxy through a 2.7×4 arcsec^2 aperture, obtaining a 14 per cent contribution from an FC at 5000 Å. Kay (1994) estimated an FC contribution of 35 per cent to the flux at 4400 Å, while Tran (1995a) found 27 per cent at 5500 Å. Mrk 348 is one of the Seyfert 2 galaxies that had a hidden Seyfert 1 nucleus revealed by spectropolarimetry (Miller & Goodrich 1990).

The Ws and continuum ratios of this galaxy are shown in Fig. 10. The Ws have values similar to those of an S4 template, without any noticeable gradient in the inner 8 arcsec. From the results of Koski (1978), Kay (1994) and Tran (1995a), we would expect the Ws to be substantially diluted in the nuclear region, but this is not detected. One possibility would be that the FC is extended, diluting *all* the Ws. However, the narrow-line region of this galaxy is extended by less than 2 arcsec (Schmitt & Kinney 1996), and the FC would have to be extended by ≈8 arcsec.

The continuum ratios show a gradient, having values similar to those of an S4 template at the nucleus and becoming bluer farther out, reaching values similar to those of S5–S6 templates. The continuum behaviour of Mrk 348 is intriguing, due to the fact that outside the nucleus it indicates bluer templates than those expected from the analysis of the Ws. This behaviour is also seen in many other objects in the present sample, particularly Seyfert 2s.

Mrk 573. Pogge & De Robertis (1993) found excess near-UV emission, spatially extended along the [O III] emission, interpreted as scattered nuclear continuum. Koski (1978) estimated that the FC contributes 12 per cent of the light at 5000 Å, observed through a 2.7×4.0 arcsec^2 aperture, while Kay (1994) finds 20 per cent FC at 4400 Å within an aperture of $\approx 2 \times 6$ arcsec^2. She also estimated, based on spectropolarimetry, that the FC is polarized by 5.6 per cent in the 3200–6300 Å range, in agreement with the values found by Martin et al. (1983).

The Ws (Fig. 11) show a mild gradient, from an S3 template at the nucleus to a bluer one, S4, at 5 arcsec. The continuum ratios show a gradient from an S3–S4 template at the nucleus to a bluer one, S5–S6, at 5 arcsec. Koski (1978) and Kay's (1994) estimations of the FC contribution to the nuclear spectrum are not confirmed by our data, which do not show any detectable dilution in the Ws. This galaxy is another case in which the continuum ratios outside the nucleus have values bluer than we would expect from the analysis of Ws.

IC 1816. This galaxy was identified as a Seyfert 1 by Fairall (1988), but the lack of variability led Winkler (1992) to question this classification. Our spectrum does not show broad emission lines, which led us to classify it as a Seyfert 2. The Ws of this galaxy (Fig. 12) have values typical of S3 templates in the inner 4 arcsec, with an *apparent* dilution in Mg caused by contamination by [N I] emission. The Ws decrease to values of an S5 template at 8 arcsec from the nucleus. The continuum ratios have values corresponding to templates bluer than the Ws, S5 at the nucleus changing to S6 at 8 arcsec.

ESO 417-G6. Our spectrum was obtained with the slit oriented along the extended emission (north-west–south-east, according to Mulchaey et al. 1996). The Ws show no gradient (Fig. 13), having values typical of an S3 template. The *apparent* dilution in the Mg band is due to contamination by [N I] emission. The continuum ratios show a gradient, changing from S3 at the nucleus to a bluer S5 template at ≈5 arcsec from the nucleus.

Mrk 607. According to De Robertis & Osterbrock (1986a) the nuclear spectrum of this galaxy shows high-excitation lines, like [Fe VII] and [Fe X], but only narrow permitted lines. Kay (1994) obtained a 10 per cent FC contribution to the nuclear flux, and estimates a 4.3 per cent continuum polarization in the 3200–6300 Å range.

The Ws and continuum ratios (Fig. 14) indicate similar templates, S2–S3 at the nucleus, S5 at 6 arcsec, suggesting a weak star-forming ring, and S3 farther out. Our spectrum of this edge-on galaxy was obtained with the slit positioned along the major axis, which may explain the large variations in the Ws in such small scales. Considering these variations, we cannot evaluate whether the nuclear Ws are diluted or not.

NGC 1358. The nuclear FC contributes 17 per cent of the flux and is polarized by 1.7 per cent in the 3200–6300 Å range, according to Kay (1994). The Ws of NGC 1358 (Fig. 15) show no systematic gradient and have values typical of an S1 template, the same result as obtained by Storchi-Bergmann & Pastoriza (1989). The only exception is Ca K, which reaches values larger than S1 at $r = -6$ arcsec. The continuum ratios show a gradient from values typical of an S1 template at the nucleus to bluer values typical of an S5 template farther out. This galaxy is another case in which the continuum ratios outside the nucleus have values bluer than those expected from the analysis of the Ws.

NGC 1386. The Ws are typical of an S3 template at the nucleus (Fig. 16), S4–S5 at 10 arcsec from the nucleus, due to the presence of spiral arms (Storchi-Bergmann et al. 1996b), and S3 farther out. The continuum ratios indicate an S1 template at the nucleus, with a gradient to values typical of S5–S6 at 10 arcsec and outwards.

CGCG 420-015. This galaxy was classified as Seyfert 2 by de Grijp et al. (1992). The W values are indicative of an S3 template at the nucleus, with the G band and Mg showing a small gradient to S2 farther out, consistent with a small dilution in the nucleus (Fig. 17). The continuum ratios indicate an S1 template at the nucleus, redder than the value predicted from the Ws, with a gradient to S3–S4 at 4 arcsec and farther out. Care must be taken when analysing the Ws and continuum ratios of this galaxy, because it was observed with the slit positioned almost perpendicular to the parallactic angle, introducing large differential refraction effects.

ESO 362-G8. The Ws are similar to an S5–S6 template at the nucleus, with a gradient to S4–S5 at 4 arcsec and farther out (Fig. 18). The continuum ratios are similar to an S5 template at the nucleus, changing to bluer values, typical of S6–S7 templates, farther out. The Ws of this galaxy indicate bluer templates in the nuclear region, which is due to the presence of young stars, revealed by strong H I absorption features. This galaxy also has continuum ratios outside the nucleus bluer than the values predicted from the Ws.

Mrk 1210. Tran, Miller & Kay (1992) found polarized broad Hα and Hβ components in the spectrum of this galaxy. Later Tran (1995a,b,c) confirmed this result and determined that the FC contributes 25 per cent of the nuclear flux at 5500 Å, while Kay (1994) estimates a 64 per cent FC contribution at 4400 Å. Nevertheless, the Ws show almost no gradient indicative of such a dilution (Fig. 19). The Ws correspond to S4 and S5 templates. The continuum ratios are similar to S5–S6 at the nucleus, with a gradient to S6 farther out, which is bluer than the template estimated from the Ws. There is an *apparent* dilution of the Mg and Na features in the nuclear spectrum due to emission-line contamination by [N I] and He I respectively.

NGC 3081. This galaxy was classified as a Seyfert 2 by Phillips et al. (1983). According to Pogge (1989), the [O III] image is

symmetrical but more extended than the stellar profile. The W profiles (Fig. 20) do not show any evidence of a stellar population gradient, with values similar to S2–S3 templates. The continuum ratios show a gradient from an S2–S3 template at the nucleus, to S4–S5 at 5 arcsec and farther out, bluer than the values indicated by the Ws.

IRAS 11215−2806. This galaxy was classified by de Grijp et al. (1992) as a Seyfert 2. The Ca K and G-band Ws (Fig. 21) present a gradient from an S4 template at the nucleus to S2 in the outer regions, indicating dilution by a blue continuum. Mg presents almost no gradient, with values typical of S3–S4 templates. The continuum ratios present a gradient in the opposite direction, from S4 at the nucleus, to S5 farther out.

MCG-05-27-013. This galaxy was classified as Seyfert 2 by Terlevich et al. (1991). The Ws of Ca K are typical of an S3 template at the nucleus, changing to S1 farther out, which suggests dilution by an FC (Fig. 22). The G band has a smaller gradient, with values similar to an S2 template at the nucleus and S1 farther out, while for Mg the values are similar to an S2 template, with no gradient. The continuum ratios have values larger than S1 at the nucleus, due to strong reddening, changing to values similar to S4 in the outer regions, bluer than the values predicted by the analysis of the Ws.

Fairall 316. This is a Seyfert 2 galaxy discovered by Fairall (1981). The Ws show no gradient (Fig. 23), with Ca K having values typical of S2, while the G band and Mg have values typical of S1. The continuum ratios have the values of an S1 template at the nucleus, decreasing outwards to values bluer than those predicted by the Ws, similar to an S3 template.

NGC 5135. NGC 5135 was described by Phillips et al. (1983) as having a *composite* nucleus with characteristics of both Seyfert 2 and starburst. Thuan (1984) obtained *IUE* spectra of this galaxy, confirming the dual nature of the nucleus, which presents both emission lines typical of Seyfert 2s and absorption lines typical of starbursts, the latter component contributing 25 per cent of the total UV emission.

The Ws (Fig. 24) show a gradient from values typical of an S7 template at the nucleus to S6–S5 at 7 arcsec. The continuum ratios also show a gradient from S6 at the nucleus to S5 at 7 arcsec. This gradient is due to the presence of young stars in the nuclear region, as revealed by strong He I absorption features.

NGC 5643. This galaxy was classified by Phillips et al. (1983) as a low-luminosity Seyfert 2. Schmitt et al. (1994) presented [O III] and Hα images, as well as optical spectra of NGC 5643. The images show the high-excitation gas to be extended along the east–west direction by ≈20 arcsec. The stellar population is moderately old in the central region, showing evidence of absorption lines diluted by a blue continuum, supposed to be scattered nuclear light.

The Ws of this galaxy present a mild gradient to the east of the nucleus (i.e. towards negative r in Fig. 25), suggesting the presence of scattered light up to at least 4 arcsec from the nucleus. In the outer regions, the Ws correspond to S3–S4 templates, while the continuum ratios correspond to S3 to the east of the nucleus and S1 to the west. Bonatto et al. (1989) obtained that the nuclear stellar population of this galaxy can be represented by an S3 template, similar to our result.

NGC 6300. Storchi-Bergmann & Pastoriza (1989) observed the nuclear stellar population of this galaxy to be old, with a small contribution from intermediate-age stars. The Ws do not show a clear gradient (Fig. 26), with Ca K varying between S2 and S3 templates, while the G band and Mg vary between S4 and S5. The continuum ratios decrease from values much larger than those of an S1 template at the nucleus to values typical of an S6 template at 10 arcsec and farther out, bluer than the values predicted from the Ws in this region.

NGC 6890. Storchi-Bergmann et al. (1990) studied the nuclear optical spectrum of this galaxy, finding that the stellar population is old and that Hα may have a broad component. The Ws show a gradient in Ca K and the G band, which change from S4 at the nucleus to S3 in the outer regions, but not in Mg, which has values typical of an S3 template, with no gradient (Fig. 27). The continuum ratios have values larger than S1 at the nucleus, decreasing to S2 in the outer regions. These results are similar to those obtained by Storchi-Bergmann et al. (1990).

NGC 7130. Like NGC 5135, this galaxy has a Seyfert 2 nucleus surrounded by a starburst (Phillips et al. 1983). Thuan (1984) presented *IUE* spectra which show both high-excitation emission lines typical of Seyfert 2s and absorption lines typical of starbursts. The starburst component dominates the UV emission, with ≈75 per cent of the flux. Shields & Filippenko (1990) showed that the narrow-line region has two kinematical components and emission-line ratios which vary from those of AGN in the nucleus to those typical of H II regions farther out.

Both Ws and continuum ratios show a marked gradient (Fig. 28). The Ws change from values similar to S7 at the nucleus to S6 farther out, while the continuum ratios change from S6–S7 at the nucleus to S5–S6 farther out. This gradient is due to the presence of a circumnuclear star-forming region.

NGC 7582. Morris et al. (1985) found circumnuclear Hα emission in this Seyfert 2 galaxy, suggesting a ring of rotating H II regions in the galaxy plane. The Ws of this galaxy show a dilution, changing from S7 at the nucleus to S3–S4 in the outer regions (Fig. 29). The continuum ratios are similar to S3 at the nucleus and north-east ($r < 0$), but decrease to values similar to S5–S6 towards $r > 0$. The continuum ratios to the south-west are bluer than what we would expect from the W results. The dilution measured in this object is probably due to its inner star-forming ring.

4.1.3 Radio galaxies

3C 33. This is an FRII radio source. Koski (1978) estimated that the FC contributes 19 per cent of the flux at 5000 Å, observed through a 2.7×4 arcsec^2 aperture. Antonucci (1984) obtained spectropolarimetric data, which show wavelength-independent polarization, but no broad polarized emission lines.

The Ws of this radio galaxy (Fig. 30) have values similar to an E3 or E6 template, although W(Mg I) is more similar to an E1 template. The continuum is redder at the nucleus, with values of an E2 template, decreasing to values typical of an E3 or E6 template farther out. The FC contribution estimated by Koski (1978) would produce a dilution of the Ws in the nuclear region. Our data do not support this result, as the W profiles are essentially flat.

PKS 0349−27. The Ws (Fig. 31) do not show a gradient and have values typical of an E1–E2 template, whereas the continuum ratios show a gradient from an E2 template at the nucleus to a bluer, E3–E4 template farther out.

Pictor A. This is an FRII broad-line radio galaxy with a strong double-lobed radio source oriented along the east–west direction (Christiansen et al. 1977). Halpern & Eracleous (1994) detected double-peaked Balmer lines, not present in previous spectra. The Ws and continuum ratios (Fig. 32) show a strong dilution by the FC at the nucleus. Their values correspond to an S4 template in the outer regions, except for the G band, where the values are similar to those of an S1 template in the outer regions. The remarks about

the uncertain continuum and W measurements in the nucleus of MCG-02-33-034 also apply to Pictor A.

PKS 0634−20. This is an FR II radio source. Simpson, Ward & Wilson (1995) did not detect a broad Paα line and showed that the $K-L$ colour, [O III] and soft X-ray fluxes are consistent with the spectral energy distribution of a quasar absorbed by $A_V \approx 30$ mag. The Ws (Fig. 33) are consistent with an E2 stellar population, without a gradient. The continuum ratios indicate bluer templates, E3 at the nucleus, decreasing to values typical of E6 farther out.

PKS 0745−19. According to Baum & Heckman (1989), this narrow-line radio galaxy does not have a well-defined FR class. The Ws indicate an E8 template at the nucleus, with a gradient to values typical of E4 farther out (Fig. 34), suggesting dilution by an FC. The continuum ratios indicate a redder, E2 stellar population. However, it should be noted that these continuum ratios were not corrected by foreground reddening, because this galaxy lies too close to the Galactic plane ($b < 4°$).

4.1.4 LINERs and normal galaxies

NGC 1326. Storchi-Bergmann et al. (1996b) obtained narrow-band [O III] and Hα images, which reveal a circumnuclear ring at $|r| \approx 6$ arcsec. As for NGC 1097 and other galaxies containing star-forming rings, the Ws and colour profiles of this galaxy (Fig. 35) confirm the presence of a ring. The radial behaviour of the Ws and continuum ratios does not suggest the presence of an FC in the nucleus. The Ws have values typical of an S3 template at the nucleus, S6 at the ring and S2–S3 farther out. The continuum ratios indicate an S1 template at the nucleus (redder than the one indicated by the Ws), S6 at the ring, and S3–S4 farther out.

NGC 1598. According to Phillips et al. (1984), the nuclear spectrum of this galaxy is similar to that of a LINER, with evidence of young stars at the nucleus, which is also surrounded by a ring of H II regions. The Ws and continuum ratios (Fig. 37) indicate similar templates: S7 at the nucleus, in agreement with the presence of young stars, and S5 from 4 to 6 arcsec, reaching values typical of an S6 template farther out.

NGC 2935. This is a normal galaxy with a nuclear ring of star formation (Buta & Crocker 1992). The Ws of Ca K and the G band are similar to S4 at the nucleus, S5 at the ring (5 arcsec) and S2 farther out, while Mg is similar to S2 at the nucleus, S3 at the ring and S2 farther out (Fig. 39). The continuum ratios are similar to S3 at the nucleus, S5 at the ring and S3 farther out.

NGC 4303. This is a Sersic–Pastoriza galaxy, classified as a LINER by Huchra, Wyatt & Davis (1982). Filippenko & Sargent's (1985) observations show that H II regions are prominent in the nucleus and circumnuclear region. They also found a substantially broader component in each line and proposed that we are seeing a faint Seyfert 2 or LINER nucleus hidden by H II regions.

The Ws are similar to an S5 template at the nucleus, decreasing to values similar to an S6 template at the ring (5 arcsec; Fig. 40). From 7 to 15 arcsec from the nucleus the Ws are similar to an S4 template, decreasing to S6–S7 in the outer regions. The continuum ratios behave like the Ws, with the exception of the nucleus and ring, where they indicate redder templates, S4 and S5 respectively. In the other regions, Ws and continuum ratios indicate similar templates. Our results are in good agreement with those of Bonatto et al. (1989).

IC 4889. Phillips et al. (1986) found Hα, [N II] and [O II] emission in this normal elliptical galaxy. The Ws show no significant gradient, with values typical of an E1 template, while the continuum ratios are E1 at the nucleus and decrease to values similar to those of an E3 template in the outer regions (Fig. 41).

NGC 5248. Both Ws and continuum ratios show the presence of a ring at $|r| = 10$ arcsec from the nucleus (Fig. 42). The values of Ca K and the G band are typical of an S5 template at the nucleus, S6 at the ring and S4 at 15 arcsec from the nucleus, decreasing to values typical of S6–S7 templates farther out. Mg and continuum ratio values indicate redder templates, S4 at the nucleus, S5 at the ring and S2–S3 at 15 arcsec, decreasing to S5–S6 farther out. Our result for the nuclear stellar population is similar to that one obtained by Bonatto et al. (1989).

NGC 6221. This southern spiral galaxy was classified as a Seyfert 2 by Véron, Véron & Zuiderwijk (1981) and Pence & Blackman (1984), based on the detection of a faint broad Hβ component and an [O III] line broader than Hβ, and on the proximity to a hard X-ray source (Marshall et al. 1979; Wood et al. 1984). However, Schmitt & Storchi-Bergmann (1995) recently proposed that the identification of NGC 6221 with the X-ray source is probably wrong and that it is more likely to be related to the high-excitation Seyfert 2 galaxy ESO 138-G01. Pence & Blackman's (1984) data also show that the nucleus is surrounded by a starburst.

Our W profiles (Fig. 43) show a gradient from an S7 template at the nucleus to S5 at 5 arcsec and farther out, in agreement with the presence of a nuclear starburst, confirmed by the gradient also observed in the continuum ratios, which correspond to S6 at the nucleus and to S5 at 5 arcsec and farther out.

5 DISCUSSION

The present set of high-quality long-slit spectra contains a wealth of information on the properties of AGN and of the stellar population of their host galaxies. In this section we discuss some of the global results revealed by our analysis and their possible implications.

5.1 Stellar populations

The values of the continuum colours and Ws of the stellar lines found in our analysis cover a wide range, as can be seen in Figs 3–44. Even in inner regions of the bulge not affected by circumnuclear star formation or by a non-stellar FC, the galaxies exhibit substantial differences in the Ws and colours, reflecting a variety of stellar population properties. This is confirmed by our characterization of the spectra in terms of Bica's (1988) templates, which shows that, despite a predominance of S2 and S3 templates, every spectral type from S1 to S7 appears in the representation of the spectra in the inner regions of our sample galaxies.

This observed *variety* of stellar population properties illustrates the inadequacy of using a single starlight template to evaluate and remove the stellar component from AGN spectra. The importance of an accurate evaluation of the starlight component cannot be underestimated. A 'template mismatch' affects not only the derived emission-line fluxes, but also, and more strongly, the determination of the strength and shape of a residual FC. We have seen, for instance, that many of the nuclei in the present sample show no evidence for dilution of the stellar lines in comparison with off-nuclear spectra of the same galaxy. However, some dilution would most probably be measured if a different galaxy were used as a starlight template. The cases of Mrk 348, 573, 1210 and 3C 33 are illustrative in this respect. Whereas Koski (1978), Kay (1994) and Tran (1995a) obtained large contributions of an FC by comparing their spectra with a normal galaxy template (Section 4.1), we find little evidence for dilution of the absorption lines by comparing the

Table 4. Column 3 lists the range in distances from the nucleus used to compute $W_{\text{off-nuc}}$. Columns 4–6 list the FC fractions corresponding to the Ca K, G-band and Mg lines respectively.

DILUTION FACTORS

Object	Type	r [arcsec]	$f_{\text{FC}}(\lambda)$ [per cent]		
			3930 Å	4301 Å	5176 Å
NGC 1097	Lin-1	4.0	6±5	–	–
NGC 1598[c]	Lin	4.0	73±4	39±6	39±6
NGC 7213	Lin-1	3.6–7.2	31±4	33±6[b]	–
ESO 362-G18	1	7.0–12.0	46±6	59±5[b]	22±6[a]
NGC 6814	1	5.0–10.8	47±4	53±6[b]	22±5[a]
MCG-02-33-034	1	4.0–7.0	76±5	100[b]	100[a]
NGC 6860	1	4.0–7.0	51±4	64±6[b]	50±5
Pictor A	BLRG	3.7–6.5	77±3	100[b]	100[a]
Mrk 348	2	1.9–3.7	1±5	9±6	9±7[a]
Mrk 1210	2	4.0–8.0	11±6	12±7	26±7[a]
IC 1816	2	4.0	13±5	15±6	30±5[a]
ESO 362-G8[c]	2	4.0–7.0	25±6	15±7	11±5
NGC 1358	2	4.0–6.0	0±5	1±7	–
NGC 5643	2	3.6–5.4	19±4	33±6	33±4[a]
NGC 6890	2	1.8–3.6	17±5	39±7	–
CGCG 420-015	2	2.0–4.0	4±5	15±6	5±7[a]
IRAS 11215-2806	2	4.0–7.0	24±4	34±5	30±5[a]
MCG-05-27-013	2	4.0–7.0	10±5	12±7	–
NGC 5135[c]	2-SB	3.6–7.2	37±8	51±7	36±8[a]
NGC 7130[c]	2-SB	3.6–7.2	47±5	62±6	35±5[a]
NGC 7582[c]	2-SB	4.0–8.0	70±4	60±6	57±5[a]
NGC 6221[c]	SB	3.6–5.4	52±4	73±4	49±6[a]
PKS 0745-19	NLRG	1.9	55±13	3±20	15±11[a]

[a]Contamination by [Fe VII] and/or [N I].
[b]Contamination by broad Hγ.
[c]Dilution due to young stars in the nucleus.

nuclear Ws with those measured a few arcseconds outside the nucleus.

This raises the question of which is the best way to estimate the stellar component in an AGN spectrum. By far the most commonly adopted procedure is to use the spectrum of a normal galaxy as a starlight template. Given the variety of stellar populations found in AGN, if a template galaxy is to be used at all then it has to be chosen from a library that contains a large variety of stellar population characteristics. An alternative technique, implicitly used in this paper, is to use an off-nucleus spectrum of the object as the starlight template. This is arguably a more robust method, as the best representation of the stellar population in a given galaxy is the galaxy itself! The extrapolation to zero radius, however, involves the assumption that the stellar population in the bulge of the host galaxy does not change dramatically in the inner few arcseconds. A comparison between these two methods of starlight evaluation will be presented in a future communication.

5.2 Dilution factors

Figs 3–44 demonstrate that several galaxies show signs of dilution of the stellar lines in the nucleus. In this section we compare the nuclear Ws with those a few arcseconds outside the nucleus in order to estimate the fraction of the continuum associated with a featureless spectral component.

In order to obtain Ws representative of the neighbourhood of the nucleus we have co-added typically four extractions, two at each side of the nucleus, located at distances ranging from 2 to 12 arcsec (see Table 4). Extractions adjacent to the nucleus were avoided whenever possible, since, due to seeing, they are often contaminated by the nuclear spectrum. The typical distance of the off-nuclear extractions was 4 arcsec, corresponding to physical radii between ~0.5 and 2 kpc for the distances of the galaxies in the sample.

After constructing these off-nuclear templates and measuring their Ws, the FC fraction of the total continuum spectrum at the wavelength of an absorption line was estimated by

$$f_{\text{FC}}(\lambda) = \frac{W_{\text{off-nuc}} - W_{\text{nuc}}}{W_{\text{off-nuc}}}, \quad (1)$$

where W_{nuc} and $W_{\text{off-nuc}}$ are the Ws in the nucleus and in the off-nuclear template respectively.

Table 4 presents the results of this analysis. Galaxies not listed in Table 4 show no signs of dilution, and even for some objects in the table (e.g. NGC 1097, Mrk 348) the evidence for dilution is only marginal – by 'marginal' we mean within 2σ of a spurious dilution caused by the errors in the W measurements. We recall that dilution of the Ws by less than 10 per cent cannot be reliably detected with this method, owing to the errors in the Ws. We concentrated this analysis on the Ca K, G-band and Mg lines. However, as indicated in the table, the Mg line is very often contaminated by [Fe VII] and/or [N I] in the nuclear spectrum, producing an *apparent* dilution. In such cases the $f_{\text{FC}}(5176\,\text{Å})$ fractions have to be taken as upper limits of the actual dilution. The line that is least affected by such spurious effects is Ca K. Empty slots in Table 4 occur whenever an increase in the W, instead of dilution, was observed.

Of the broad-lined objects in our sample, only NGC 526a does not exhibit a systematic dilution of the Ws in the nucleus. The other

possible exception is NGC 1097, which does show some dilution in the Ca K line, but at a marginal level. The highest values of f_{FC} occur for MCG-02-33-034 and Pictor A, where it reaches nearly 80 per cent at the wavelength of Ca K. However, as discussed in Section 3, these values are not as reliable as for other Seyfert 1s, owing to the uncertain positioning of the continuum for these two objects. Indeed, their nuclear spectra are so complex that the G-band and Mg lines are completely filled by emission, preventing a determination of f_{FC} at the corresponding wavelengths.

Perhaps the most intriguing aspect of Table 4 is the low degree of dilution detected in Seyfert 2s. Of the 20 Seyfert 2s in our sample, 13 are listed in Table 4, and only nine of these (IC 1816, ESO 362-G8, NGC 5135, 5643, 6890, 7130, 7582, MCG-05-27-013 and IRAS 11215-2806) have dilution convincingly detected. As reviewed in Section 4.1, NGC 5135, 7130, 7582 and ESO 362-G8 are composite nuclei, showing features of both Seyfert 2s and starbursts. In these cases, as for the LINER NGC 1598 (Fig. 37), the dilution is almost certainly dominated by the young stellar component, not a genuine AGN continuum. This lowers the count to five objects with detected dilution out of 16 'pure' Seyfert 2s. Marginal indications of dilution were found in Mrk 348, Mrk 1210, NGC 1358 and CGCG 420-015. In the other objects, the FC, if present at all, contributes 10 per cent or less in the optical. This result is further discussed below.

5.2.1 *Implications for FC2*

The low level or lack of dilution in Seyfert 2s found in the present analysis is an interesting result in light of the current debate over the existence and origin of a FC in Seyfert 2s and its implications for unified models. It has been shown that the FC in Seyfert 2s cannot be simply the continuum of a hidden AGN scattered into our line of sight, otherwise broad emission lines should also be seen, in contradiction with the very definition of type 2 Seyferts (Cid Fernandes & Terlevich 1992, 1995; Heckman et al. 1995). Furthermore, the low levels of polarization (Miller & Goodrich 1990) and the observation of reflected broad lines substantially more polarized than the FC (Tran 1995c) are also in conflict with the simple obscuration/reflection picture.

These facts lead to the idea that a *second* FC component (dubbed FC2 by Miller 1994) must be present in Seyfert 2s. The nature of this component remains unknown, although both a circumnuclear starburst (Cid Fernandes & Terlevich 1995; Heckman et al. 1995) and free–free emission from the scattering region (Tran 1995c) have been suggested.

Our observations seem to indicate that an FC (and consequently FC2) is *not* a universal phenomenon in Seyfert 2s, and that previous determinations of the FC strength have been overestimated. A smaller FC contribution would alleviate, if not completely solve, all the problems listed above.

A good way to investigate this issue further would be to obtain spectropolarimetry for the Seyfert 2s in the present sample. We expect galaxies for which no dilution of the Ws was detected to show little or no polarization. IC 1816, NGC 5643, NGC 6890, MCG-05-27-013 and IRAS 11215−2806, on the other hand, should exhibit large polarizations and Seyfert 1 features in the polarized spectra. In the cases of composite nuclei, spectropolarimetry could help to disentangle the starburst and Seyfert 2 components and possibly reveal a hidden AGN.

As a final word of caution, we note that while throughout this paper we have attributed the dilution of absorption lines in the nuclei of active galaxies to an FC, dilution can also be caused by young stars, as shown to occur in circumnuclear star-forming rings (e.g., Figs 3, 36 and 38) and in the nuclei of the starburst galaxies NGC 6221 and 7130 (Figs 43 and 28). It is a known problem in optical spectroscopy of AGN that it is often difficult to distinguish between a young stellar population and an FC (e.g. Miller & Goodrich 1990; Cid Fernandes & Terlevich 1992; Kay 1994). UV spectroscopy offers the most direct way of removing this ambiguity (e.g. Leitherer, Robert & Heckman 1995; Heckman et al. 1995).

5.2.2 *Metallicity gradients*

In measuring the dilution of absorption lines with respect to their strengths ∼4 arcsec (or ∼1 kpc) outside the nucleus, we are making the assumption that the stellar population in the bulge of the host galaxy does not change appreciably from $r \sim 4$ arcsec to $r = 0$. This approximation might not be valid if the galaxy presents a strong metallicity (Z) gradient, leading to an increase of the Ws towards the nucleus (e.g. Díaz 1992). If such a gradient is present, then a flat W profile such as the one found in many of our galaxies could reflect the compensating effects of an FC diluting the enhanced metal lines in the nucleus.[1] In this section we investigate this possibility by means of an approximate treatment of the potential effects of a metallicity gradient.

To estimate the Z-gradient we have used $\Delta \log Z/\Delta \log r = 0.2$, a typical value obtained for $r \gtrsim 3$ arcsec in elliptical galaxies (Davies, Sadler & Peletier 1993 and references therein). Assuming that the nuclear stellar population sampled in our 2×2 arcsec^2 aperture is characterized by a mean radius of 0.5 arcsec, and considering a typical off-nuclear extraction distance of 4 arcsec, this corresponds to an increase of ∼0.2 dex in Z from $r = 4$ arcsec to the nucleus, corresponding to the inner ∼1 kpc of the galaxy. This value is also typical of Z-gradients mapped from the radial variations of the O abundances in H II regions in galactic discs (e.g. Vila-Costas & Edmunds 1992 and references therein). To convert this gradient to a W-gradient we used the results of Jablonka, Alloin & Bica (1992). We adopted their calibration for an old, globular cluster population, corresponding to the steepest W–Z relation, thus resulting in the largest possible W-variations for a fixed Z-gradient.

This exercise resulted in the following variations of the Ws owing to a Z-gradient: ΔW(Ca K) = 1.2 Å, ΔW (G band)= 0.8 Å and ΔW(Mg) = 0.5 Å. Given that the assumptions above were all made in the sense of maximizing the effects of a Z-gradient, these variations should be regarded as upper limits. These are small variations, being of the same order as the errors in the W (Section 3.1). The net variations with respect to the typical values of the W found in our off-nuclear extractions (∼13 Å for Ca K and ∼8 Å for both the G band and Mg) would correspond to changes of, at most, 10 per cent in W(Ca K), 8 per cent in W(G band) and 6 per cent in W(Mg).

These results, while certainly not closing the question, seem to indicate that Z-gradients do not constitute a serious caveat to the interpretation of W profiles in AGN. Only galaxies with an FC weaker than 6–10 per cent could have a dilution of the metal lines masked by the Z-gradient. Whilst we do not think that the compensating effects of an FC and a Z-gradient provide a viable interpretation for the ubiquitous absence of dilution in our sample galaxies, particularly in Seyferts 2, further work on the strength and detectability of Z-gradients in active galaxies would clearly be welcome, as this issue also bears on the question of whether an

[1] We thank Dr R. Terlevich for pointing this out to us.

off-nuclear extraction provides a better starlight template for the nuclear stellar population than a normal galaxy (Section 5.1).

5.3 Colour gradients

The continuum ratios in the sample galaxies exhibit an interesting radial behaviour. As seen in Figs 3–44, the F_{5870}/F_{4020} and F_{4630}/F_{3780} ratios very often peak in the nucleus, indicating a *redder* continuum. This seems to be an extremely ubiquitous behaviour. The two kinds of objects that do not follow this rule are those containing nuclear starbursts, namely NGC 1598, 6221, 5135 and 7130, and broad-lined objects, the most extreme examples being MCG-02-33-034 and Pictor A. In particular, *all* Seyfert 2s, with the exception of NGC 5643 which shows a complex colour profile, have nuclei redder than the extranuclear regions. This effect is not an artefact of our pseudo-continuum determination, as we verified that the colour profiles are nearly identical if instead of the pseudo-continuum one defines line-free bands close to the pivot-points to compute mean fluxes and flux ratios.

This is a somewhat surprising result, given that the general prejudice is that AGN are bluer than normal galaxies, and as such they should also be bluer than their own bulges. On the other hand, if taken as evidence of reddening, the colour profiles would fit into the currently favoured view that the nuclear regions of Seyfert 2s are rich in dust. Some support to this interpretation comes from the behaviour of the Na line (partially produced in the interstellar medium), whose W profiles in some galaxies, notably ESO 417-G6, NGC 1386, ESO 362-G8, NGC 6300 and NGC 7582, peak in the nucleus, mimicking the colour profiles. Examination of the radial behaviour of the Hα/Hβ emission-line ratio would provide a test of this interpretation.

Another intriguing result was found from the comparison of the stellar population templates inferred from the Ws with those inferred from the continuum ratios for the Seyfert 2s. With few exceptions, the off-nuclear colours indicate a spectral template *bluer* than that indicated by the absorption lines. At present we cannot give a clear explanation for this apparent contradiction, but we speculate on two possible interpretations. (1) The effect is due to a strong contribution from metal-rich (thus strong-lined) intermediate-age (thus blue) stars, a population not well represented by any of templates S1–S7. This would be a genuine stellar population effect. (2) The blue continuum is due to a scattered AGN component while the absorption lines originate in a metal-rich population. This would result in an *extended dilution* of the stellar features, whose Ws would therefore be underestimated, leading to the incorrect attribution of a spectral template less metallic than the actual population. Detailed modelling will be required to test these possibilities.

6 SUMMARY

We have reported the results of a high signal-to-noise ratio long-slit spectroscopy study of 38 active galaxies and four normal galaxies. The run of stellar absorption lines and continuum colours with distance from the nucleus was investigated using a consistent methodology, aiming at a global characterization of the stellar populations and the detection of a nuclear FC through the dilution of conspicuous absorption lines with respect to off-nuclear extractions. Our results can be summarized as follows.

(1) Radial variations of the stellar populations were detected in most cases. Star-forming rings, in particular, were found to leave clear imprints in the equivalent widths and colour profiles.

(2) The stellar populations in the inner arcseconds of active galaxies are varied, as inferred from the wide spread of equivalent widths and colours measured in this work. This fact alone raises serious doubts as to whether it is appropriate to use a single starlight template to evaluate and remove the stellar component from AGN spectra.

(3) The equivalent width profiles were used to measure the dilution of the absorption lines in the nucleus with respect to off-nuclear spectra. Dilution by a nuclear FC was detected in most broad-lined objects in the sample.

(4) Galaxies undergoing star formation in their nuclei, including composite starburst + Seyfert 2 objects, also show dilution of the nuclear absorption lines. The dilution in these cases is due to young stars, not to an FC. These galaxies also show a clear colour gradient, their nuclei being bluer than their off-nuclear regions.

(5) About 50 per cent of the Seyfert 2s in the sample show no signs of dilution of their absorption lines in the nucleus, indicating that an FC, if present, contributes less than 10 per cent of the total flux in the optical range. Possible consequences to the (controversial) nature of the FC in Seyfert 2s were discussed.

(6) All but one of the Seyfert 2s present a colour gradient in the sense that the spectrum gets *redder* as we approach the nucleus, indicative of the presence of dust.

(7) There is an apparent discrepancy between the spectral templates assigned from the equivalent widths of the absorption lines and from the continuum colours, an effect observed in the off-nuclear spectra of most Seyfert 2s in the present sample. Tentative interpretations involving either a stellar population effect or an extended blue continuum were briefly outlined.

ACKNOWLEDGMENTS

We thank Dr E. Bica for useful discussions and remarks on an early version of this manuscript. HRS acknowledges the hospitality of the Department of Physics at Florianópolis. Support from FAPEU-UFSC is also duly acknowledged. RCF's work was partially supported by CNPq under grant 300867/95-6. This research has made use of the NASA/IPAC Extragalactic Database (NED), which is operated by the Jet Propulsion Laboratory, Caltech, under contract with the National Aeronautics and Space Administration. The Cerro Tololo Interamerican Observatory is operated by the Association of Universities for Research in Astronomy, Inc., under contract with the National Science Foundation.

REFERENCES

Antonucci R. R. J., 1984, ApJ, 278, 499
Baum S. A., Heckman T., 1989, ApJ, 336, 681
Bica E., 1988, A&A, 195, 76
Bica E., Alloin D., 1986, A&A, 166, 83
Bica E., Pastoriza M. G., da Silva L. A. L., Dottori H., Maia M., 1991, AJ, 102, 1702
Bica E., Alloin D., Schmitt H., 1994, A&A, 283, 805
Bonatto C. J., Bica E., Alloin D., 1989, A&A, 226, 23
Buta R., 1986, ApJS, 61, 631
Buta R., Crocker D. A., 1992, AJ, 103, 1804
Christiansen W. N., Frater R. H., Watkinson A., O'Sullivan J. D., Lockhart I. A., 1977, MNRAS, 181, 183
Cid Fernandes R., Terlevich R., 1992, in Filippenko A., ed., ASP Conf. Ser. Vol. 31, Relationships between Starburst and Active galaxies. Astron. Soc. Pac., San Francisco, p. 241
Cid Fernandes R., Terlevich R., 1995, MNRAS, 272, 423
Davies R. L., Sadler E. M., Peletier R. F., 1993, MNRAS, 262, 650

de Grijp M. H. K., Keel W. C., Miley G. K., Goudfrooij P., Lub J., 1992, A&AS, 96, 389
De Robertis M. M., Osterbrock D. E., 1986a, ApJ, 301, 98
De Robertis M. M., Osterbrock D. E., 1986b, ApJ, 301, 727
Díaz A. I., 1985, PhD thesis, University of Sussex
Díaz A. I., 1992, in Filippenko A., ed., ASP Conf. Ser. Vol 31, Relationships between Starburst and Active galaxies. Astron. Soc. Pac., San Francisco, p. 181
Fairall A. P., 1981, MNRAS, 196, 417
Fairall A. P., 1988, MNRAS, 233, 691
Filippenko A. V., Halpern J. P., 1984, ApJ, 285, 458
Filippenko A. V., Sargent W. L. W., 1985, ApJS, 57, 503
Filippenko A. V., Sargent W. L. W., 1988, ApJ, 324, 134
Fosbury R. A. E., Mebold U., Goss W. M., Dopita M. A., 1978, MNRAS, 183, 549
Garcia-Vargas M. L., Díaz A. I., Terlevich R., Terlevich E., 1990, Ap&SS, 171, 65
Halpern J. P., Eracleous M., 1994, ApJ, 433, L17
Halpern J. P., Filippenko A. V., 1984, ApJ, 285, 475
Heckman T. et al., 1995, ApJ, 452, 549
Ho L. C., Filippenko A. V., Sargent W. L. W., 1993, ApJ, 417, 63
Huchra J. P., Wyatt W. F., Davis M., 1982, AJ, 87, 1628
Jablonka P., Alloin D., Bica E., 1990, A&A, 235, 22
Jablonka P., Alloin D., Bica E., 1992, A&A, 260, 97
Kay L. E., 1994, ApJ, 430, 196
Keel W. C., 1983, ApJ, 269, 466
Kinney A. L., Bohlin R. C., Calzetti D., Panagia N., Wyse R. F. G., 1993, ApJS, 86, 5
Koski A. T., 1978, ApJ, 223, 56
Leitherer C., Robert C., Heckman T., 1995, ApJS, 99, 173
Lípari S., Tsvetanov Z., Macchetto F., 1993, ApJ, 405, 186
McQuade K., Calzetti D., Kinney A., 1995, ApJS, 97, 331
Malkan M. A., Filippenko A. V., 1983, ApJ, 275, 477
Marshall F. E., Boldt C. A., Holt S. S., Mushotzky R. F., Pravdo S. H., Rotschild R. E., Serlemitsos P. J., 1979, ApJS, 40, 657
Martin P. G., Thompson I. B., Maza J., Angel J. R. P., 1983, ApJ, 266, 470
Miller J. S., 1994, in Bicknell G. V., Dopita M. A., Quinn P. J., eds, ASP Conf. Ser. Vol. 54, The First Mount Stromlo Symposium: The Physics of Active Galaxies. Astron. Soc. Pac., San Francisco, p. 149
Miller J. S., Goodrich R. W., 1990, ApJ, 355, 456
Morris S., Ward M., Whittle M., Wilson A. S., Taylor K., 1985, MNRAS, 216, 193
Mouri H., Taniguchi Y., Kawara K., Nishida M., 1989, ApJ, 346, L73
Mulchaey J. S., Wilson A. S., Tsvetanov Z., 1996, ApJS, 102, 309
Osterbrock D. E., De Robertis M. M., 1985, PASP, 97, 1129
Pence W. D., Blackman C. P., 1984, MNRAS, 207, 9
Phillips M. M., 1979, ApJ, 227, L121
Phillips M. M., Charles P. A., Baldwin J. A., 1983, ApJ, 266, 485
Phillips M. M., Pagel B. E. J., Edmunds M. G., Díaz A. I., 1984, MNRAS, 210, 701
Phillips M. M., Jenkins C. R., Dopita M. A., Sadler E. M., Binette L., 1986, AJ, 91, 1062
Pogge R. W., 1989, ApJ, 345, 730
Pogge R. W., De Robertis M. M., 1993, ApJ, 404, 563
Ruiz M., Rieke G. H., Schmitt G. D., 1994, ApJ, 423, 608
Schmitt H. R., Kinney A. L., 1996, ApJ, 463, 497
Schmitt H. R., Storchi-Bergmann T., 1995, MNRAS, 276, 592
Schmitt H. R., Storchi-Bergmann T., Baldwin J. A., 1994, ApJ, 423, 237
Sekiguchi K., Menzies J. W., 1990, MNRAS, 245, 66
Sérsic J. L., Pastoriza M., 1965, PASP, 77, 287 (SP65)
Sérsic J. L., Pastoriza M., 1967, PASP, 79, 152 (SP67)
Shields J. C., Filippenko A. V., 1990, AJ, 100, 1034
Stauffer J. R., 1982, ApJ, 262, 66
Simpson C., Ward M. J., Wilson A. S., 1995, ApJ, 454, 683
Storchi-Bergmann T., Pastoriza M. G., 1989, ApJ, 347, 195
Storchi-Bergmann T., Bica E., Pastoriza M. G., 1990, MNRAS, 245, 749
Storchi-Bergmann T., Baldwin J. A., Wilson A. S., 1993, ApJ, 410, L11
Storchi-Bergmann T., Eracleous M., Halpern J., Wilson A., Filippenko A., 1995a, ApJ, 443, 617
Storchi-Bergmann T., Kinney A. L., Challis P., 1995b, ApJS, 98, 103
Storchi-Bergmann T., Wilson A. S., Baldwin J. A., 1996a, ApJ, 460, 252
Storchi-Bergmann T., Rodriguez-Ardila A., Schmitt H. R., Wilson A. S., Baldwin J. A., 1996b, ApJ, 472, 83
Storchi-Bergmann T., Bica E., Kinney A., Bonatto C., 1997, MNRAS, 290, 231
Terlevich R., Melnick J., Mesagosa J., Moles M., Copetti M. V. F., 1991, A&AS, 91, 285
Thuan T. X., 1984, ApJ, 281, 126
Tran H. D., 1995a, ApJ, 440, 565
Tran H. D., 1995b, ApJ, 440, 578
Tran H. D., 1995c, ApJ, 440, 597
Tran H. D., Miller J. S., Kay L. E., 1992, ApJ, 397, 452
Véron M. P., Véron P., Zuiderwijk E. J., 1981, A&A, 98, 34
Véron-Cetty M.-P., Véron P., 1986, A&AS, 66, 335
Vila-Costas M. B., Edmunds M. G., 1992, MNRAS, 259, 121
Winge C., Peterson B. M., Horne K., Pogge R. W., Pastoriza M., Storchi-Bergmann T., 1995, ApJ, 445, 680
Winkler H., 1992, MNRAS, 257, 677
Wood K. S. et al. 1984, ApJS, 56, 507
Yee H. K. C., 1980, ApJ, 241, 894

This paper has been typeset from a TEX/LATEX file prepared by the author.